JPET Fast Forward. Published on April 2, 2019 as DOI: 10.1124/jpet.119.256537
This article has not been copyedited and formatted. The final version may differ from this version.

Effects in cancer cells of the recombinant L-Methionine gamma-lyase from *Brevibacterium aurantiacum.* Encapsulation in human erythrocytes for sustained L-methionine elimination

David Machover, Luigia Rossi, Jocelyne Hamelin, Christophe Desterke, Emma Goldschmidt, Bernadette Chadefaux-Vekemans, Pascal Bonnarme, Pierre Briozzo, David Kopečný, Francesca Pierigè, Mauro Magnani, Rosella Mollicone, Farhad Haghighi-Rad, Yann Gaston-Mathé, Julien Dairou, Claude Boucheix, and Raphaël Saffroy.

Affiliations: Assistance Publique-Hôpitaux de Paris, Hospital Paul-Brousse, Villejuif, France (D.M., E.G., R.S, J.H.); INSERM U935, Villejuif, France (D.M., F.H.-R., C.D., C.B.); University Paris-Sud, Villejuif, France (D.M., R.M., J.H., F.H.-R., C.D., R.S., C.B.); University Paris-Saclay, Paris, France (D.M., R.M., J.H., F.H.-R., C.D., R.S., C.B.); University of Urbino *Carlo Bo*, Urbino, Italy (L.R., F.P., M.M.); INSERM U1193, Villejuif, France (J.H., R.S.); INSERM U1197, Villejuif, France (R.M.); INRA-AgroParisTech, UMR 782 GMPA, Thiverval-Grignon, France (P.Bo.); Institut Jean-Pierre Bourgin, INRA-AgroParisTech, University Paris-Saclay, Versailles, France (P.Br.); CRH-Department of Protein Biochemistry and Proteomics, Palacký University, Olomouc, Czech Republic (D.K.); YGM Consult SAS, Paris, France (Y.G.-M.); CNRS UMR 8601, Paris, France (J.D.); Assistance Publique-Hôpitaux de Paris, Hospital Necker-Enfants Malades, Paris. France (B.C.-V.); and University Paris-Descartes, Paris, France (J.D., B.C.-V.).

Running title: Methionine gamma-lyase from *B. aurantiacum* in cancer cells

Corresponding author: David Machover, MD. Department of Medical Oncology. Hospital Paul-Brousse. 94800 Villejuif. France. Telephone: +33 (0)609436331. Fax: +33 (0)145593498. E-mail address: david.machover1@orange.fr ; david.machover@aphp.fr

Number of pages including Title and Running title pages, Abstract, main text, and Footnote page: 19

Number of tables: 4

Number of figures: 10

Number of references: 42

Number of words in Abstract: 203

Number of words in Introduction: 325 including reference citations

Number of words in Discussion: 1,454 including reference citations

Supplemental section including 1 table, and 1 figure.

Abbreviations used in the text: MGL, L-methionine γ-lyase; PLP, pyridoxal 5'-phosphate; PN, pyridoxine; PM, pyridoxamine; SAM, S-adenosyl L-methionine; UL, unloaded cells.

Recommended section assignment: Chemotherapy, Antibiotics, and Gene Therapy.

Abstract

Methionine deprivation induces growth arrest and death of cancer cells. To eliminate L-methionine we produced, purified and characterized the recombinant pyridoxal 5'-phosphate (PLP)-dependent L-methionine gamma-lyase MGL-BL929 from the cheese-ripening *Brevibacterium aurantiacum*. Transformation of an *Escherichia coli* strain with the gene *BL929* from *B. aurantiacum* optimized for *E. coli* expression led to production of the MGL-BL929. Elimination of L-methionine and cytotoxicity *in vitro* were assessed, and methylation-sensitive epigenetics was explored for changes resulting from exposure of cancer cells to the enzyme. A bioreactor was built by encapsulation of the protein in human erythrocytes to achieve sustained elimination of L-methionine in extracellular fluids. Catalysis was limited to α,γ-elimination of L-methionine and L-homocysteine. The enzyme had no activity on other sulfur-containing amino acids. Enzyme activity decreased in presence of serum albumin or plasma resulting from reduction of PLP availability. Elimination of L-methionine induced cytotoxicity on a vast panel of human cancer cell lines and spared normal cells. Exposure of colorectal carcinoma cells to the MGL-BL929 reduced methyl-CpG levels of hyper methylated gene promoters including that of CDKN2A whose mRNA expression was increased, together with decrease in global histone H3-dimethyl lysine9. The MGL erythrocyte bioreactor durably preserves enzyme activity *in vitro* and strongly eliminates L-methionine from medium.

Introduction

Methionine deprivation in cancer cells induces growth arrest and cell death, whereas normal cells are much more resistant (Halpern et al., 1974; Hoffman and Erbe, 1976; Stern et al., 1984). Depletion of L-methionine can be achieved by methionine gamma-lyases (L-methionine-α-deamino-γ-mercaptoethane-lyase; MGL), pyridoxal 5'-phosphate (PLP) enzymes that catalyse α,γ-elimination of L-methionine resulting in production of methanethiol, α-ketobutyrate, and ammonia. Various MGLs have been obtained by extraction or by recombination of genes from bacteria, protozoa and plants (Dias and Weimer, 1998; Sun et al., 2003; Sato and Nozaki, 2009; Tokoro et al, 2003). The MGL from *Pseudomonas putida* (*P. putida-MGL*) exerts cytotoxicity in most tumor cell lines *in vitro*, and enhances the effect of 5-fluorouracil (FUra). Potentiation is accompanied by changes of folate pools (Machover et al., 2001) and by decrease in DNA methylation (Machover et al., 2002). Enhancement of FUra, cisplatin, and bis (2-chloroethyl)-nitrosourea cytotoxicity by *P. putida-MGL* was described in mice given repeated injections of *P. putida-MGL* (Yoshioka et al. 1998; Kokkinakis, 2006). However, attempts at reducing anaphylaxis of the native *P. putida-MGL* in primates through polyethylene glycol (PEG) conjugation resulted in substances with unstable activity that slowed down its use in humans (Sun et al., 2003; Yang et al., 2004).

We hypothesized that immunogenicity of any MGL derived from parasitic and potential pathogenic microorganisms would not allow systemic administration to humans in safe conditions (Sato and Nozaki, 2009). Moreover, excepting for the L-methionine γ-lyase from the plant *Arabidopsis thaliana* (Goyer et al., 2007), other MGLs as yet characterized including that engineered from human cystathionine γ-lyase, eliminate L-cysteine whose deficiency may cause undesirable effects (Sato and Nozaki, 2009; Stone et al, 2012; Kudou et al., 2008; Hori et al., 1996). The recombinant MGL-BL929 presented herein is derived from *Brevibacterium aurantiacum,* a microorganism abundantly present in food, this MGL having a possibility for human oral immune tolerance (Forquin et al., 2011; Steele et al., 2012). Furthermore, MGL-BL929 substrates are restricted to L-methionine and its precursor, L-homocysteine.

Materials and Methods

Source of the recombinant L-methionine γ-lyase BL929. The enzyme MGL-BL929 originates from *Brevibacterium aurantiacum* (strain *ATCC 9175*), a cheese ripening microorganism characterized by release of typical cheese aroma, and orange pigment production. *Brevibacteriaceæ* reach proportions greater than 5% of bacteria in a number of cheese varieties.

Studies of gene expression by transcriptome analysis in *B. aurantiacum* in presence of L-methionine showed up-regulation of two adjacent genes, including a gene encoding for a methionine transporter (*metPS*) and the gene *BL929* (Forquin et al., 2011). Up-regulation of *BL929* was

accompanied by production of volatile compounds resulting from degradation of methionine. The sequence *BL929* was identified within the genome of *Brevibacterium linens* BL2 described in the Integrated Microbial Genomes & Microbiomes system (https://img.jgi.doe.gov/) under Locus Tag BlinB01000978. The sequence *BL929* is composed of 1182 base pairs (Table 1, Sequence 1) corresponding to a translated protein of 393 residues (Table 1, Sequence 2). Protein sequence alignment (Clustal Omega; https://www.ebi.ac.uk/Tools/msa/clustalo/) showed identity rates ranging from 27.4% to 40.1% between the MGL-BL929 and other described methionine γ-lyases (e.g., percent identity was 27.4, 37.4, 37.2, 33.1, 33.7, 37.8, 36.7, 36.7, 38.2, 39.3, 37.5, 37.2, 40.1, and 38.5 between the MGL-BL929 and the MGLs from *Arabidopsis thaliana, Aeromonas hydrophila sp., Entamœba histolytica 1 and 2, Pseudomonas putida, Trichomonas vaginalis 1 and 2, Citrobacter freundii, Porphyromonas gingivalis, Treponema denticola, Fusobacterium nucleatum, Clostridium novyi,* and *Clostridium sporogenes,* respectively).

Production and purification of MGL-BL929. The open reading frame (ORF) encoding MGL-BL929 was optimized to adapt *B. aurantiacum* codon usage to *Escherichia coli* expression (Table 1, Sequence 3). The optimized sequence flanked with restriction sites for endonucleases *Nde*I and *Xba*I was synthesized and then subcloned in the *E. coli* pGTPc608 expression vector (pET9d derivative including PTac promoter, Lac operator, Laclq, multiple cloning sites, and T1T2 terminator; GTP Technology, Labège, France), according to GeneArt procedures (GeneArt, Regensburg, Germany). Plasmids (pGTPc608-BL929) were verified by digestion and sequencing (GeneArt).

A single colony of *E. coli* BL21 (DE3) production strain (Agilent Technologies, Santa Clara, CA) transformed with the pGTPc608-BL929 plasmid was grown in a 50-liter Applikon bioreactor containing 35 l of GYP medium (yeast extract 24 g/l, soy peptone 12 g/l, KH_2PO_4 4.8 g/l, K_2HPO_4 2.2 g/l and glycerol 5 g/l) supplemented with PLP 0.02% (w/v). Expression was induced with IPTG when the OD_{600nm} of the culture reached 2. Concentrated feeding solution (30% w/v glycerol and 30% w/v yeast extract) was added with a remote controlled pH flow-regulated pump. Cells were harvested when the culture reached OD_{600nm} of 40-50.

Cells were suspended in 20 mM Tris-HCl, 1mM PMSF, 1mM EDTA, 1mM DTT, 0.1 mM PLP, pH 7.5, and lysed by high pressure homogenization. The MGL-BL929 was purified from cell extracts by chromatography in five steps consisting in one hydrophobic interaction chromatography and then two successive sequences of anion exchange chromatography followed by endotoxin removal. Briefly, cell extracts were clarified by centrifugation, and then filtered through a 0.45 µm low level protein binding filter (Sartorius, Göttingen, Germany). Ammonium sulphate (AS) was added to the cell extracts to a final concentration of 0.75 M. After centrifugation at 4°C, and then filtration through a 0.45 µm low level protein binding filter, cell extracts were injected in a column of Phenyl Sepharose (High Sub) 6 Fast Flow resin (GE Healthcare Europe, Vélizy, France). The column was equilibrated with 20 mM

Tris-HCl, 0.75 M AS, 0.1 mM PLP, pH 7.5, and proteins were eluted by stepwise decrease in AS concentration. Elution fractions were pooled, concentrated using an ultra-filtration cassette with a 10 kDa cut-off (Pall, Port Washington, NY), and then diafiltered versus 7 volumes of 20 mM Bis-tris, 0.1 mM PLP, pH 6.0. Elution fractions were passed through a column of DEAE Sepharose Fast Flow resin (GE Healthcare) equilibrated in 20 mM Bis-tris, 0.1 mM PLP, pH 6.0. Proteins were eluted by increasing NaCl concentration from 0 to 1 M. Elution fractions were concentrated using an ultra-filtration cassette, and then diafiltered versus 7 volumes of 40 mM sodium phosphate buffer, PLP, 20 µM, pH 7.5. Elution fractions were filtered with a 0.2 µm low level protein binding filter (Corning, Union City, CA) and then endotoxins were removed using a High Capacity Endotoxin Removal column (HCER, Thermo Pierce). Sequential DEAE Sepharose and HCER chromatography was repeated once. Protein fractions were concentrated to 50-80 mg/ml. Enzyme concentration and purity were determined by Bradford assay, capillary electrophoresis and SDS PAGE. Endotoxin levels were assessed by Lonza (Testing Services). Purified MGL-BL929 in solution of 40 mM sodium phosphate buffer, 100 mM NaCl, and 20 µM PLP, pH 7.5, was stored at -80°C.

Characterization. Oligomerisation was assayed by Size Exclusion Chromatography (SEC) using a Superdex 200 5/150 GL column (GE Healthcare).The ability of purified MGL-BL929 to catalyse elimination reactions was assessed with L-methionine, L-homocysteine, L-cysteine, L-cystathionine, S-adenosyl L-homocysteine, and D-methionine. Enzyme ≥ 95% pure was diluted in 100 mM potassium phosphate buffer, 0.01 mM PLP; pH 7.5, and 25 mM of substrate. The mixture was incubated at 37°C for 5 minutes and sampled. The reaction was stopped by addition of trichloroacetic acid to a final concentration of 5%, and then α-ketoacid formed was measured with 3-methyl-2-benzothiazolone hydrazone (MBTH) using spectrophotometry at 320 nm (Takakura et al., 2004). Kinetics for α,γ-elimination catalysis was assessed with L-methionine and L-homocysteine. Studies of enzyme stability were done with the purified MGL-BL929 incubated at 37°C in phosphate-buffered saline (PBS); PBS with human serum albumin (HSA) at 40 g/l; pure human plasma; and pure rat plasma, each of these containing 4 different concentrations of PLP up to 200 µM (Figure 1). Enzyme activity was measured at t_0, and after 8 hours and 24 hours of incubation. Enzyme activity was assessed at 25°C in PBS. Experiments were done in quadruplicate. Western blots were performed in each condition at each time of incubation. Western blot analysis for estimation of apoenzyme levels under various conditions was done by SDS-PAGE probed with rabbit MGL-BL929 antiserum (Eurogentec, Angers, France). The reaction was revealed with anti-rabbit IgG alkaline phosphatase conjugate, and visualized with Western Blue Substrate (Promega); sensitivity was 0.1 µg/ml of protein.

Effects of MGL-BL929 in cell culture. L-Methionine concentration changes were assessed in supernatant of HT29, SKOV3, JURKAT, and REH human cancer cells exposed to MGL-BL929 in

various concentrations (Figure 2). Measurement was done by ultra-performance liquid chromatography tandem mass spectrometry (UPLC-MS/MS; Waters, Milford, MA) using L-methionine-(methyl)-D_3 as internal standard (Watervall et al., 2009). A panel of 35 human cancer cell lines originating from various cell types (American Type Culture Collection, Manassas, VA) was used to determine the cytotoxicity spectrum of MGL-BL929 (Table 2). Cells were thawed from mycoplasma-free frozen stocks and were controlled for contamination. Cytotoxicity against non-cancer cells was explored using primary 533 skin fibroblasts from a normal child, and fibroblasts from an individual with Congenital Disorder of Glycosylation II (CDG-II). Cells were grown in standard RPMI 1640 or DMEM culture media, supplemented with 10% FBS and antibiotics at 37°C in an atmosphere with 5% CO_2, and were exposed to the MGL-BL929 for 72 h in 12-well cell plates. Viability was measured using flow cytometry. Living cells were defined by light double scatter, and counted in a BD Accuri C6 flow cytometer (BD Biosciences, Le-Pont-de-Claix, France). Each experiment was done in duplicate. Cell growth inhibition data were analyzed according to the median-effect principle for concentration-effect analysis. Dose-effect plots including 50% inhibitory concentrations (IC_{50}) and 95% confidence intervals were obtained with the CalcuSyn v2 software (Biosoft, Cambridge, UK).

Assessment of methylation-related epigenetic changes in human colorectal cancer cells exposed to MGL-BL929.

Quantitation of 5-methylcytosine (5-meC) in DNA from gene promoters. Changes of 5-methylcytosine (5-meC) levels within CpG dinucleotide fragments from gene promoters containing 5-meC baseline levels greater than 70% were quantitatively assessed in HT29 cells exposed to MGL-BL929 at 1 Unit/ml, and at 2 Unit/ml for 24h, 48h, and 72h. The MassARRAY System (Agena Bioscience, Hamburg, Germany) was used for quantitative methylation analysis of bisulfite-treated genomic DNA from 50 selected CpG sites from promoter sequences of 39 genes described as having hyper methylated promoter regions in colon cancer cell lines (Ehrich et al., 2008). Genomic DNA was extracted from cells using a QIAamp DNA mini kit (Qiagen, Courtabœuf, France). Concentration and purity of DNA were determined by absorbance using a NanoVue spectrophotometer. Sodium bisulfite DNA modification was performed using EZ DNA Methylation Kit (Zymo Research, Orange, CA, USA). The 50 amplicons and PCR primers were designed from http://agenacx.com/epidesigner/ (Supplemental Table S1). The amplification regions covered CpG islands of promoters of target genes overlapping with the DNA sequences corresponding to 5' untranslated regions (5' UTR). The target regions of the sodium bisulfite-treated genomic DNA were amplified by PCR using designed primers. Each forward primer contained a 10-nucleotide tag (5'-AGGAAGAGAG-3') to balance the PCR, and each reverse primer contained a T7 promoter tag and sequences insert (5'-CAGTAATACGACTCACTATAGGGAGAAGGCT-3') for *in vitro* transcription. Amplification

comprised an initial incubation at 94°C for 4 min, 45 cycles of denaturation at 95°C for 20s, annealing at 62°C for 30s, extension at 72°C for 1 min, and final incubation at 72°C for 3 min. Unincorporated dNTPs were dephosphorylated with premix for *in vitro* transcription including shrimp alkaline phosphatase (Agena Bioscience). The reaction mixture was incubated at 37°C for 40 min before phosphatase heat inactivation. PCR product was then subjected to *in vitro* transcription with RNase-A cleavage for the T-reverse reaction. Samples were spotted onto a 384-pad Spectro-CHIP using MassARRAY NanoDispenser, and spectra were acquired with MassARRAY compact MALDI-TOF mass spectrometer (Agena Bioscience). Methylation calls were analysed with EpiTYPER software (Agena Bioscience) to quantitate results for each CpG site. Results were expressed in percent methyl-CpG change between cells unexposed to the enzyme and cells exposed to each concentration of MGL-BL929 at same times of growth. Statistical comparisons of the difference between percent methylation in paired samples were done with two-sided Wilcoxon Rank-Sum Test. One-way ANOVA was used to study differences in methylation rates according to time of cell culture in unexposed cells, and to time of enzyme exposure in treated cells. Statistical analysis was done with the R software, v3.4.4.

Quantitation of mRNA gene expression by Real-Time Reverse Transcription-PCR. Changes in mRNA expression of four genes by Real-time reverse transcription-PCR were quantitatively assessed in HT29 and in HCT116 colon cancer cells exposed to MGL-BL929 at 1 Unit/ml, and at 2 Unit/ml for 48 hours and 72 hours. We selected three genes whose promoter CpGs were partially demethylated under MGL-BL929 in HT29 cells (CDKN2A; ATP10A; and MyoD) as presented below, and one gene (DNM1L) that was not assessed for changes of 5-meC levels because its promoter was not reported to be hyper methylated in colorectal cancer cells (Ehrich et al., 2008). The Cyclin-dependent kinase inhibitor 2A (CDKN2A) gene encodes proteins that mainly regulate the Retinoblastoma susceptible gene product (pRb) and p53 pathways that play critical roles for cell cycle and apoptosis (Li et al., 2011). Down regulation is frequently involved in oncogenic processes (Herman et al., 1995; Hinshelwood et al., 2009; Li et al., 2011). MyoD gene encodes for a myogenic factor that is expressed in skeletal muscle lineage and is repressed in other tissues (Buckingham and Rigby, 2014). The ATP10A encodes a protein of the P-type cation transport ATPase family, and the DNM1L gene product belongs to the dynamin family of large GTPases. Messenger RNA of target genes (CDKN2A, MyoD, ATP10A, and DNM1L) and of endogenous reference genes (S18 rRNA, and β-Actin) from HT29 and HCT116 cells was used for cDNA synthesis. Amounts of cDNA from target and reference genes obtained by PCR amplification under each experimental condition were determined from standard curves constructed with cDNA from the hepatocellular carcinoma MAHLAVU cells. Total RNA was extracted using Qiagen kit (Qiagen). Complementary DNA was synthesized using QuantiTect Reverse Transcription reagents including DNase treatment (Qiagen) mixed with RNA. Cycling conditions were 42°C for 30 min, followed by denaturation at 95°C for 3 min. PCR amplification was performed on the LightCycler 480 instrument (Roche Applied Science, Mannheim,

Germany), and data were analyzed with the LightCycler 480 Software, v1.5. PCR was performed with QuantiFast Sybr-Green PCR Master Mix reagents (Qiagen) for CDKN2A, and S18, and with QuantiFast Probe PCR Master Mix reagents for MYOD1, ATP10A, DNM1L, β-Actin, and S18 for mRNA quantitation. One µl of reverse transcription product was used for each round of PCR. One µl of pure and diluted ($1/10^{th}$; $1/100^{th}$; $1/1{,}000^{th}$) cDNA from MAHLAVU cells was used for standard curves. Enzyme was activated by incubation at 95°C for 5 min. Each of the 50 PCR cycles consisted of a denaturation step at 95°C for 30 seconds, and then hybridization of probes and primers and DNA synthesis at 60°C for 90s. Experiments were done in duplicate. Quantitative data of both S18 rRNA and β-Actin mRNA obtained under each condition were used as endogenous housekeeping references for normalization. The amount of target was divided by that of reference gene to obtain a normalized ratio value. Relative expression level (as n-fold change) was obtained by dividing normalized ratio values obtained with cells exposed to the MGL-BL929 under each condition by the normalized ratio in control cells unexposed to the enzyme at same time point (Bièche et al., 1998).

Expression of the protein $p16^{INK4A}$ in cancer cells. Expression of the protein $p16^{INK4A}$, a product of the CDKN2A gene, was assessed by Western blot in the HT29, and HCT116 colon carcinoma, and in the HeLa cervix adenocarcinoma cells exposed to the MGL-BL929 at 1 Unit/ml for 48 hours, and in cells unexposed to the enzyme. We chose to test the effect of the MGL-BL929 on p16 translation only at 1 U/ml for 48 hours with the aim at avoiding any possible deleterious effect of excessive L-methionine elimination on protein synthesis under higher concentration of enzyme and longer times of exposure. The $p16^{INK4A}$ primarily functions in cell cycle control as a negative regulator of the pRb-E2F pathway; it specifically inhibits at the G1 to S transition the cyclin-dependent kinases 4 (CDK4) and 6 (CDK6)-mediated phosphorylation of pRb (Li et al., 2011). After trypsinisation, cells were lysed in Laemmli buffer, sonicated on ice, and then centrifuged at 4°C. Protein samples were transferred to a Low-fluorescence PVDF Transfer membrane (GE Healthcare) at 40 volt overnight. After blocking for 90 min in Tris buffer saline, 5% BSA, and 0.1% Tween 20, blots were probed with rabbit antibodies against $p16^{INK4A}$ from two sources (anti CDKN2A/p16INK4a 108349, Abcam, Cambridge, UK; and anti p16INK4a 1D7D2, ThermoFisher Scientific, Illkirch, France), and against actin. Membranes were imaged with the LI-COR Odyssey Infrared Imaging System (LI-COR Biosciences, Bad Hombourg, Germany), and band intensities were quantified with the LI-COR Odyssey software. Comparisons were performed between cells unexposed to the MGL-BL929 and those exposed to the enzyme at same time points. Two separate experiments were done.

Quantitation of dimethylated Histone H3-lysine levels by Western blot. To explore the influence of L-methionine deprivation on histone methylation, we quantitated global histone H3-dimethyl lysine levels by Western blot in HT29 and HCT116 cells exposed to the MGL-BL929 at 1 Unit/ml, and at 2 Unit/ml for 48 hours, and 72 hours. Cells were lysed in Laemmli buffer, sonicated on

ice, and then centrifuged at 4°C. Protein samples were transferred to a Low-Fluorescence PVDF Transfer Membrane, and then probed with antibodies against histone H3 dimethylated on different lysines (H3K4me2; H3K9me2; H3K27me2; H3K36me2; H3K79me2), and against total histone H3 (Methyl-Histone H3 Ab Sampler Kit 9847S; Cell Signaling Technology, Leiden, The Netherlands). Membranes were imaged with the LI-COR Odyssey Infrared Imaging System. Band intensities were quantified with the LI-COR Odyssey software and compared to that in control cells unexposed to MGL-BL929 at same time point.

Assessment of plasma L-methionine depletion and enzyme levels in mice given parenteral native MGL-BL929. Measurement of L-methionine levels (Watervall et al., 2009) and Western blots were done in plasma after a single injection of enzyme in groups of three mice per dose of enzyme and time point. Female C57Bl/6 mice aged 6 weeks were given MGL-BL929 i.p. at 50 Unit or 200 Unit per mouse. Female Balb/C mice aged 6 weeks were given the enzyme i.v. at 50 Unit per mouse. Blood was drawn 1, 3, 6, and 24 hours after injection.

Construction of a heterologous bioreactor by encapsulation of the MGL-BL929 in human erythrocytes. With the aim at preserving MGL function for long periods of time in vivo, we constructed a heterologous bioreactor by encapsulation of the MGL-BL929 in human erythrocytes. These cells internalize L-methionine and have the capacity to synthesize PLP, the cofactor required to preserve the intracellular activity of the PLP-dependent L-methionine γ-lyase (Zempleni and Kübler, 1994; Machover et al., 2018). Carrier erythrocyte lifespan does not differ from, or is only slightly shorter than that of intact cells (Bax et al., 1999), a characteristic that allows maintaining therapeutic blood levels of loaded cells for prolonged periods of time. Moreover, carrier erythrocytes prevent loaded proteins to be released in the extracellular environment and are progressively degraded in the organism by the mononuclear phagocytic system without producing toxic substances. Human blood was obtained from healthy adults and collected in heparin. Recombinant MGL-BL929 was loaded into erythrocytes by sequential hypotonic dialysis, isotonic resealing and reannealing as previously described (Magnani et al., 1988), with slight modifications. Erythrocytes were first washed twice at 4°C in solution A (154 mM NaCl, 10 mM HEPES-NaOH, 5 mM glucose, and 200 μM PLP; pH 7.4). Then, cells were suspended at 50 % erythrocyte volume fraction in encapsulation solution consisting of solution A supplemented with various concentrations of MGL-BL929 ranging from 11 Unit/ml to 270 Unit/ml. Hypotonic hemolysis was performed by dialysis of 1 ml of cell suspension in a cellulose tube (cutoff 14 kDa) versus 50 ml of 60 mOsm hypotonic solution (Fiske 210 micro sample Osmometer, Norwood, MA) consisting in 10 mM $NaHCO_3$, 10 mM NaH_2PO_4, 20 mM glucose, 2 mM ATP, 3 mM glutathione and 200 μM PLP; pH 7.4, for 90 min at 4°C. At the end of dialysis, osmolality of cell suspensions was approximately 90 mOsm. Erythrocyte resealing and reannealing were performed by incubating ten volumes of cell suspension in one volume of hypertonic solution of

100 mM inosine, 100 mM sodium pyruvate, 33 mM NaH_2PO_4, 1.66 M KCl, 190 mM NaCl, 10 mM glucose, 20 mM ATP, 4 mM $MgCl_2$, and 200 μM PLP; pH 7.4 (approximately 3,900 mOsm) for 25 min at 37°C. Finally, after three gentle washes in solution A at 4°C, cells were suspended in this solution and used for experiments. Enzymatic activity (Unit of MGL per ml of packed cells) was measured in loaded cells obtained immediately after encapsulation and at various times after loading (Takakura et al., 2004). Morphologic parameters of loaded erythrocytes were assessed at various times after the loading procedure. These included optical morphologic study, and measurement of red cell parameters (Hematology Analyzer Coulter Ac T 5diff. Beckman Coulter, Miami, FL). Estimation of anaerobic glycolysis by measurement of lactate production (μmol/hr/ml of packed cells; GEM Premier 3000 Analyzer, Instrumentation Laboratory, Bedford, MA) was carried out immediately after the encapsulation procedure. Western blot analysis (sensitivity, 0.1 μg/ml of protein, *i.e.*, approximately 0.6 mUnit/ml) was performed in cell supernatant of encapsulated cells at various times of incubation to control for release of free MGL-BL929 from loaded cells. Unloaded (UL) erythrocyte suspensions (*i.e.*, cells subjected to encapsulation procedure without enzyme) and untreated cells were used as control in all experiments. Elimination of L-methionine was assessed in supernatant of erythrocytes loaded with MGL-BL929 (at 11 Unit/ml, 54 Unit/ml, or 270 Unit/ml in encapsulation solution) incubated at 0.5% cell volume fraction for up to 96 or 120 hours in media consisting of PBS (50 mM NaH_2PO_4/Na_2HPO_4, 90 mM NaCl; pH 7.4), 5 mM glucose, PLP (0.1 μM or 200 μM), and L-methionine (100 μM or 1,000 μM) at 37°C in an atmosphere containing 5% CO_2. Experiments in medium containing vitamin B6 as pyridoxine (PN) or pyridoxamine (PM) at 200 μM instead of PLP were performed to test MGL function of the bioreactor under exposure to unphosphorylated B6 vitamers (Di Salvo et al., 2011). Potency and duration of L-methionine elimination was assessed in medium supplemented with L-methionine once at t_0, twice at t_0 and after 24 hours of incubation, and three times at t_0, and after 24 hours, and 48 hours of incubation. At planned intervals up to 96 or 120 hours, 2 ml aliquots of cell suspension were used for measurement of L-methionine in supernatant (Watervall et al., 2009).

Results

Production and characterization of the recombinant MGL-BL929. Purification of MGL-BL929 was achieved to homogeneity from a 50-liter scale cell pellet. Protein more than 95% pure containing small levels of endotoxin (49.4 Endotoxin Unit/ml) was concentrated to 79.6 mg/ml. Molecular mass is 46.5 kDa and the hydrodynamic volume assessed by SEC corresponds to a 171.5 kDa globular protein, which suggests that MGL-BL929 is a monodisperse homotetrameric protein. Catalytic activity is limited to α,γ-elimination of L-methionine and L-homocysteine (Table 3). Mean K_M for L-methionine was 6.83 ± 2.45 mM and specific activity was 5.77 ± 1.4 μmol mn^{-1} mg^{-1}. The enzyme had no detectable catalytic activity towards L-cysteine, L-cystathionine, S-adenosyl-L-homocysteine and

D-methionine. The MGL-BL929 was stable at 25°C for > 24 hours without additional PLP. At 37°C, the enzyme lost 20% of its initial activity after 24 hours in PBS in the presence of ≤ 2 μM of PLP, but activity remained stable with PLP at > 20 μM (Figure 1). Activity of MGL-BL929 decreased in HSA in the absence of PLP, and augmented with increasing concentrations of cofactor at 8 hours of incubation. In pure plasma, the enzyme lost activity by ≥ 90% after 8 hours of incubation that could not be preserved by PLP up to 200 μM. Loss of activity was not accompanied by decrease of apoenzyme as estimated by Western blot.

The native MGL-BL929 eliminates L-methionine in cell culture, and exerts strong cytotoxicity in human cancer cell lines *in vitro*. L-Methionine was eliminated from supernatant of all four cell lines studied, and the effect was augmented with increasing concentrations of enzyme (Figure 2). The MGL-BL929 induced cytotoxicity against 33 of the 35 cancer cell lines tested in the panel (Table 2). In the 33 cancer cell lines that were sensitive to the MGL-BL929, cytotoxicity appeared at ≤ 0.5 Unit/ml and increased with increasing concentrations of enzyme; in these cells, IC_{50}s ranged from 0.05 Unit/ml to 2.14 Unit/ml. Resistance to methionine deprivation was only found in SW480 and SW620 colorectal cancer cells that originate respectively from the primary tumor and a metastatic site from the same tumor. Exposure of human skin fibroblasts CDGII and 533 to the enzyme affected their growth at concentrations much greater than that required for cytotoxicity of cancer cells. IC_{50} was 4.7 Unit/ml in CDG-II cells, and it was not reached at 10 Unit/ml in 533 cells.

Methylation-related epigenetic changes occurred in human colorectal cancer cells exposed to MGL-BL929. Of 50 CpG sites from 39 selected gene promoters in HT29 cells, variable numbers of fragments comprising a single CpG or groups of 2 to 5 contiguous CpGs were amplified (Table 4, Figure 3, and Supplemental Figure S1). Exposure of cells to the MGL-BL929 decreased 5-methyl-CpG levels of hyper methylated gene promoters. Differences of 5-methyl-CpG rates between paired samples from cells unexposed and exposed to enzyme were not significant after 24 hours and became highly significant after 48 hr, and 72 hr of exposure to both concentrations of enzyme studied (Table 4). No significant difference was found with one-way ANOVA in methylation rates between control cells sampled at different times of growth that were not exposed to the enzyme and were used for comparisons with cells exposed to MGL-BL929 at 1 Unit/ml ($P = 0.99$) and at 2 Unit/ml ($P = 0.17$). Significant differences in methylation rates according to time of enzyme exposure were found by one-way ANOVA in cells exposed to MGL-BL929 at 1 Unit/ml (***$P = 2\text{x}10^{-10}$) and 2 Unit/ml (***$P = 5\text{x}10^{-5}$) which indicate that 5-meC promoter DNA levels decrease with increasing time of exposure to the enzyme. With the exception of MyoD whose transcripts were not detected in HT29 and HCT116 cells, transcripts of CDKN2A, ATP10A and DNM1L were amplified in both colorectal carcinoma cells unexposed to the MGL-BL929. Exposure of these cell lines to the enzyme at 1 Unit/ml, and 2 Unit/ml for 48 hr and 72 hr resulted in marked increase in CDKN2A mRNA expression of variable

JPET Fast Forward. Published on April 2, 2019 as DOI: 10.1124/jpet.119.256537
This article has not been copyedited and formatted. The final version may differ from this version.

degree, from approximately 10- to more than 10^5-fold of that in unexposed cells at same time points (Figure 4). No change in mRNA level from that found in unexposed cells was observed for ATP10A whose promoter had been partially demethylated in HT29 cells exposed to MGL-BL929 (Figure 3, and Supplemental Figure S1), and for DNM1L. No appreciable differences in relative gene expression were observed with normalized ratios obtained either with the 18S rRNA gene (Figure 4) or the β-Actin gene (not shown). We analysed in the HT29 cell line the individual data of the 3 genes whose promoter methylation levels under exposure to the MGL-BL929 were assessed, together with mRNA expression (i.e., CDKN2A, MyoD, and ATP10A). From this analysis, we neither observed appreciable differences in mean levels of baseline CpG methylation of individual gene promoters nor in mean rates of demethylation under L-methionine depletion at the two concentrations of enzyme (1 U/ml and 2 U/ml) and times of exposure (48h and 72h) that could explain the changes observed only in CDKN2A mRNA expression. Statistical comparisons of mRNA expression levels in HT29 cells using the Student's t-test found that CDKN2A expression decreased with increasing concentration of MGL-BL929 from 1 U/ml to 2 U/ml at 48h (*P = 0.02), and at 72h of exposure (*P <0.02), as well as with increasing time of exposure to the enzyme from 48h to 72h at 1 U/ml (*P <0.02), and at 2 U/ml (*P <0.02). In HCT116 cells, statistical difference was only found for decrease of CDKN2A mRNA expression with increasing concentration of MGL-BL929 from 1 to 2 U/ml in cells exposed for 72 hours to the enzyme (*P <0.05). The effect of the MGL-BL929 on levels of CDKN2A mRNA expression (Figure 4) was greater at the lowest concentration of enzyme (*i.e.*, 1 U/ml), as it also was on DNA fragments of gene promoters successfully amplified whose number decreased with increasing concentration of the enzyme (Table 4). These observations could result from profound L-methionine depletion under exposure to MGL-BL929 at 2 U/ml below limits allowing precise analysis of changes resulting from L-methionine deprivation in cancer cells. The protein $p16^{INK4A}$ was not detected by Western blot using two different antibodies in HT29 and HCT116 cells unexposed to the MGL-BL929 (Figure 5). Expression of the protein neither occurred in cells exposed to the enzyme despite great increase of CDKN2A mRNA found in this condition. In contrast, HeLa cells strongly expressed $p16^{INK4A}$, with no appreciable change in band intensities according to enzyme exposure. Decrease in overall H3K9me2 band intensities from control ranging from 77% to 89% (mean decrease, 83%) occurred in both HT29 and HCT116 cells exposed to MGL-BL929 at 1 Unit/ml or 2 Unit/ml, except for one single smaller decrease by 38% in HT29 cells exposed to the enzyme at 1 Unit/ml for 72 hours (Figure 6). Relative band intensity changes by ± 15% in total histone H3, and in histone H3-dimethyl lysines H3K4me2, H3K27me2, H3K36me2, and H3K79me2 levels, did not occur.

Methionine elimination in mouse plasma *in vivo* with the native enzyme is effective for short periods of time. Purified MGL-BL929 at 200 Units i.p. reduced L-methionine to undetectable levels 1 hour after injection, but recovery to 60% from baseline occurred in 3 hours. At 50 Units i.p. or i.v., methionine concentration decreased to 60% from baseline one hour after injection, and decrease lasted

for 3 hours or less. Loss of effectiveness was not accompanied by appreciable changes in Western blot band intensities for apoenzyme in plasma after 24 hours from injection.

Human erythrocytes encapsulated with MGL-BL929 retain enzyme activity for long periods of time *in vitro*, and form a bioreactor with sustained MGL function that strongly eliminates L-methionine. Morphologic and functional parameters were assessed in carrier cells loaded with the enzyme and unloaded (UL) cells incubated during 96 hr in 50 mM NaH_2PO_4/Na_2HPO_4, 90 mM NaCl, 5 mM glucose, 200 μM PLP, and 100 μM L-methionine; pH 7.4 at 37°C in an atmosphere containing 5% CO_2. No change in cell number, total amount of haemoglobin (Hb), mean cell Hb (MCH), and mean cell Hb concentration (MCHC) was observed during the entire period of time. Unchanged Hb content together with absence of extracellular MGL-BL929 by Western blot in supernatant indicates that encapsulated cells do not release intracellular macromolecules. After 96 hr of incubation, both loaded and UL cells had increase in mean cell volume (MCV) and red-blood cell distribution width (RDW) by approximately 23%, and 13%, respectively, and a number of erythrocytes acquired echinocyte-like morphology. Lactate production was not modified by the process; it was 4.25, 3.75, and 4.15 μmol/h/ml of packed erythrocytes were found in untreated cells, in unloaded cells, and in cells loaded with MGL-BL929, respectively. Enzyme load in erythrocytes augmented gradually with increasing concentration of enzyme in encapsulation solution as estimated by Western blot band intensities (Figure 7). However, L-methionine γ-lyase activity within loaded erythrocytes at t_0 (in Unit/ml of packed cells) augmented with increasing concentrations of enzyme in encapsulation solution only from 11 U/ml to 54 U/ml, but did not increase further, or minimally, at 270 U/ml (Figure 7). Activity decreased partially in the long term; after 96 hours of incubation, residual MGL activity was 54%, 67%, and 29% from values at t_0 in cells loaded with 270, 54, and 11 Unit/ml of enzyme in encapsulation solution, respectively. From comparisons between enzyme activity and Western blot band intensities in erythrocytes at t_0 (Figure 7), no apparent correlation was observed between activity and protein load obtained with MGL-BL929 above 54 U/ml in encapsulation solution. Further studies are needed to explain this discrepancy.

Human erythrocytes loaded with the MGL-BL929 incubated at 0.5% erythrocyte volume fraction in medium with 50 mM NaH_2PO_4/Na_2HPO_4, 90 mM NaCl, 5 mM glucose, and 100 μM L-methionine supplemented with PLP at 200 μM, strongly eliminated L-methionine from supernatant (Figure 8). Unloaded control cells had no effect. L-Methionine elimination rates augmented with increasing enzyme load in erythrocytes encapsulated with 11 U/ml and 54 U/ml. However, elimination rates were similar with erythrocytes loaded with 270 U/ml and with those loaded with 54 U/ml; these two formulations of the bioreactor eliminated L-methionine from supernatant almost completely at 48 hours, with only minimal differences in elimination rates at 24 hours of incubation (Figure 8). Erythrocytes loaded with 11 U/ml eliminated L-methionine at lower rates than did cells with higher

concentrations of the enzyme; under this condition, residual concentrations of L-methionine in supernatant after 96 hours of incubation were approximately 10% of initial levels (Figure 8). These findings are in accordance with data of MGL activity obtained within erythrocytes (Figure 7). Initial L-methionine elimination rates were more marked from incubation medium containing PLP at 200 μM than that from medium containing PLP at 0.1 μM (Figure 9). However, gradual elimination of L-methionine was produced by MGL-BL929-loaded cells incubated in medium with the lowest concentration of PLP; in this condition, depletion was completed after 120 hr. Similar figures were found in experiments with cells incubated in medium containing pyridoxine (PN) or pyridoxamine (PM) instead of PLP (Figure 9). Potency and duration of L-methionine elimination by enzyme-loaded erythrocytes at 0.5% erythrocyte volume fraction was assessed from medium with 50 mM NaH_2PO_4/Na_2HPO_4, 90 mM NaCl, 5 mM glucose, and 200 μM PLP, supplemented with high concentration L-methionine (1 mM) once at t_0, twice at t_0 and after 24 hours, and three times at t_0, after 24 hours and after 48 hours from start of the experiment (*i.e.*, media containing cumulative amounts of L-methionine of 1 mM, 2 mM or 3 mM) (Figure 10). Elimination of these great amounts of L-methionine occurred rapidly and persisted during the 96 hours of the experiment as demonstrated in supernatant supplemented twice or three times with L-methionine. Erythrocytes loaded with MGL at 270 Unit/ml in encapsulation solution eliminated high concentration L-methionine slightly faster than did cells loaded with 54 Unit/ml, but residual methionine was less than 0.5% from control by 48 hours from start of the experiment with erythrocytes loaded with each of these two concentrations of enzyme (not shown). These findings are comparable to that with smaller concentration of L-methionine in medium (Figure 8). Elimination of L-methionine from extracellular medium was due to the ability of the reactor to internalize and then catabolize L-methionine, since enzyme was not released from cells into medium. Highly sensitive Western blot analysis of supernatants could not detect free extracellular enzyme with the exception of traces found in only rare instances of long incubation times, which are accompanied by morphologic alteration of erythrocytes.

Discussion

The MGL-BL929 exhibits the conserved homotetrameric structure found in all other methionine γ-lyases that belong to the γ-family of PLP-dependent enzymes (Sato and Nozaki, 2009; Yang et al., 2004; Sun et al., 2003; Kudou et al., 2007; Kudou et al., 2008). Protein sequence alignment showed identity rates ranging from 27.4% to 40.1% between the MGL-BL929 and other known MGLs that originate from various bacterial, protozoan, and plant sources. The MGL-BL929 is different from that encoded by the putative sequence from *Brevibacterium linens* that was previously described (Amarita et al., 2004). Using the latter sequence we obtained a recombinant protein in *E. coli* which does not possess MGL activity, and whose function remains unknown (unpublished). Our failure to produce an

MGL with this sequence is not in agreement with the reported recombinant enzyme that was obtained with the same gene in *Lactococcus lactis* (Hanniffy et al. 2009)

Substrate specificity of the MGL-BL929 restricted to L-methionine and its immediate precursor L-homocysteine has not been described for other characterized recombinant MGLs whose catalytic activity extend to various sulfur-containing amino acids or substituted amino acids (Sato and Nozaki, 2009; Stone et al., 2012; Kudou et al., 2008; Hori et al., 1996; Tokoro et al., 2003). In particular, excepting for the methionine γ-lyase from *Arabidopsis thaliana* (Goyer et al., 2007), other MGLs catalyse α,β-elimination of L-cysteine. The vast cytotoxic activity spectrum of the MGL-BL929 comprising 33 of 35 human cancer cell lines of different origin and cell type demonstrates that enzymatic exclusive methionine deprivation induces growth inhibition and cell death in most cancer cells. However, sensitivity to L-methionine depletion, whose degree depends on concentration of MGL-BL929 (Figure 2), varies among cancer cell lines resulting in IC_{50}s ranging from 0.05 U/ml to 2.14 U/ml (Table 2). It is noteworthy that amounts of MGL-BL929 producing high L-methionine elimination rates leading to concentrations close to the detection limit, lead to variable degrees of cytotoxicity. The mechanisms underlying cancer cell growth inhibition with respect to degree of L-methionine availability have not yet been determined. Resistance to methionine deprivation was only found in two colorectal cancer cell lines that originate from two different tumor sites of the same primary. These rare exceptions indicate that methionine dependence may not be a constant metabolic feature in cancer as previously suggested (Stern et al., 1984), and that growth independence with respect to exogenous methionine supply can be retained at different stages of the neoplastic evolution. Instability of the MGL-BL929 activity *in vitro* can be explained, in part, by the affinity of HSA for PLP, and by dephosphorylation of PLP by plasma alkaline phosphatases that may reduce cofactor availability (Bohney et al., 1992; di Salvo, 2011). Requirement for cofactor is likely due to weak binding of the apoenzyme to PLP, a feature that may be exhibited by most MGLs (Sun et al., 2003; Yang et al., 2004). However, differences in binding affinities of apoenzyme for cofactor between these enzymes have been reported; e.g., dissociation constant (K_D) values for binding to PLP was found 0.62 μM for the MGL from *Citrobacter freundii*, and 14.5 μM for the MGL from *Clostridium Novyi* (Kulikova et al., 2017).

Reduction of methylation levels of hyper methylated gene promoters in HT29 carcinoma cells confirms with a highly sensitive method for 5-meC quantitation prior results of global genomic DNA methylation analysis performed with the MGL from *P. putida* in CCRF-CEM lymphoma cells (Machover et al., 2002). Decrease of promoter 5-meC DNA levels with increasing time of exposure to the enzyme fits with the hypothesis of a mechanism related to progressive decrease in availability of S-adenosyl L-methionine (SAM), the cofactor of DNA methyltransferases, due to L-methionine deficiency. Results suggest that partial demethylation of CDKN2A promoter contributed to increase

mRNA expression level. However, genes needed for cell maintenance including DNM1L and ATP10A, as well as MyoD, a mesenchymal lineage specification gene that is repressed in epithelial cells, had not their mRNA expression changed even though ATP10A and MyoD promoters were partially demethylated under exposure to MGL-BL929. L-Methionine deficiency induced histone H3 dimethyl lysine level changes restricted to global H3K9me2 whose levels were strikingly reduced. These findings of selective decrease in overall H3K9me2 accompanying demethylation of a large number of highly hypermethylated gene promoters suggest triggering of a process that is not likely to be explained solely by decrease in SAM availability. Analysis of the epigenetic significance of these changes requires further experiments using chromatin immunoprecipitation (ChIP) to explore histone H3 dimethyl lysine distribution along specific genes and their relation with promoter methylation and transcription. Prior studies using this method showed that DNA methylation-dependent gene silencing is associated with gain of H3K9me2 at specific gene regions (Kondo et al., 2003; Kondo et al., 2004; Hinshelwood et al., 2009). Increased gene-associated H3K9me2 occurred with CDKN2A promoter hypermethylation and silencing in HCT116, RKO, and SW48 colorectal cancer cells (Kondo et al., 2003); and enrichment for H3K9me2 marks accompanying CDKN2A gene promoter hyper methylation was found in primary human mammary cells progressing *in vitro* from normal to pre-malignant cells (Hinshelwood et al., 2009). Absence of the $p16^{INK4A}$ suggests the presence of a process preventing this protein to be expressed in HT29 and HCT116 cells growing in standard conditions as well as under exposure to MGL-BL929. This repressive yet unidentified mechanism is cell line specific because $p16^{INK2A}$ was present in control HeLa cells. Transcription of altered CDKN2A mRNA and impairment of $p16^{INK4A}$ translation in cancer cells by several mechanisms have been reported (reviewed by Li et al., 2011). We hypothesize that cytotoxicity induced by L-methionine deficiency is related to mechanisms resulting from SAM deficiency. Within the context of gene expression complexity found in cancer cell lines, present findings suggest that the cytotoxic effect of MGL-BL929 is due, in part, to changes in methylation-sensitive epigenetic abnormalities involved in oncogenesis including DNA methylation.

Predictably from data of enzyme stability *in vitro*, duration of L-methionine depletion in mouse plasma after parenteral administration of MGL-BL929 was short, falling in the time range limits reported for the native MGL from *Pseudomonas putida* (Sun et al., 2003; Yang et al. 2004; Stone et al., 2012). Parenteral supply of PLP was found to overcome inactivation of the PEG-conjugated MGL from *P. putida* in mouse plasma (Yang et al., 2004; Sun et al., 2003), suggesting that high-dose PLP, as well as high doses of unphosphorylated B6 vitamers (e.g., PN or PM) given by parenteral route should be studied with the aim at improving stability of the native MGL-BL929 in plasma whose inactivation is, at least in part, due to insufficient cofactor availability. However, exogenous or synthesized PLP is likely to be cleared from plasma by serum albumin and alkaline phosphatases at rates that may prevent achievement of cofactor levels required to sustain activity of the MGL lying

free in plasma for long periods of time (Zempleni and Kübler, 1994; Bohney et al., 1992; di Salvo et al., 2011). From these limitations to the use of the free native enzyme, we hypothesized that carrier erythrocytes could provide encapsulated MGL-BL929 with the environment required for prolonged catalytic function. Furthermore, in this configuration, absence of α,β-elimination of L-cysteine with the MGL-BL929 should have limited or no impact on glutathione synthesis, whose deficiency would shorten enzyme-loaded erythrocyte lifespan (Meister and Anderson, 1983). As reported with the MGL from *P. putida* (Gay et al., 2017), we successfully built a bioreactor with durable catalytic MGL function by encapsulation of the MGL-BL929 into human erythrocytes. Under present experimental conditions, intracellular erythrocyte environment durably preserves MGL activity. The intense and durable elimination of high concentrations of L-methionine from medium highlights the robustness of the bioreactor whose MGL function is retained *in vitro*. The variable rapidity of L-methionine elimination according to concentration of PLP in medium is likely to be due to differences in amounts of cofactor uptake by MGL-loaded erythrocytes (Maeda et al., 1976). Furthermore, based on the naturally occurring rapid decline of PLP concentration in red blood cells (Zempleni and Kübler, 1994; Machover et al., 2018), evidence of elimination of L-methionine by the bioreactor from medium containing low concentration PLP as well as PN or PM instead of PLP, suggest that sustained MGL function within loaded erythrocytes in the longer term is likely to relate with newly synthesized intracellular cofactor (Anderson et al., 1971; di Salvo et al., 2011). These findings together with data from previously reported erythrocyte pharmacokinetics of vitamin B6 (Zempleni and Kübler, 1994; Machover et al., 2018), suggest the possibility to modulate the bioreactor's MGL activity *in vivo* by supplying cells with B6 vitamers.

Treatment of cancer with the powerful cytotoxic MGL-BL929 from *Brevibacterium aurantiacum* requires a pharmaceutical delivery system preserving activity of the enzyme in order to achieve sustained L-methionine depletion *in vivo*. Development of a bioreactor with this capacity is in progress.

Acknowledgments: We thank Dr. Ibrahim Casal for animal experimental support

Authorship Contributions

Participated in research design: Machover, Goldschmidt, Saffroy, Hamelin, Rossi, and Gaston-Mathé

Conducted experiments: Machover, Hamelin, Saffroy, Mollicone, Rossi, Pierigè, and Haghighi-Rad

Contributed new reagents or analytic tools: Machover, Bonnarme, Rossi, Pierigè, Saffroy, Hamelin, Chadefaux-Vekemans, Desterke, Magnani, Mollicone, Haghighi-Rad, Dairou, Briozzo, Kopečný, and Boucheix

Performed data analysis: Machover, Saffroy, Hamelin, Goldschmidt, Rossi, Desterke, Mollicone, Haghighi-Rad, Chadefaux-Vekemans, Pierigè, and Dairou

Wrote or contributed to the writing of the manuscript: Machover, Goldschmidt, Rossi, Bonnarme, Briozzo, Desterke, Saffroy, and Boucheix.

References

Amarita F, Yvon M, Nardi M, Chambellon E, Delettre J, and Bonnarme P (2004). Identification and functional analysis of the gene encoding Methionine-γ-lyase in *Brevibacterium linens*. *Appl Env Microbiol* 70: 7348-7354

Anderson BB, Fulford-Jones CE, Child JA, Beard MEJ, and Bateman CJT (1971). Conversion of vitamin B6 compounds to active forms in the red blood cell. *J Clin Invest* 50: 1901-1909

Bax BE, Bain MD, Talbot PJ, Parker-Williams EJ, and Chalmers RA (1999). Survival of human carrier erythrocytes *in vivo*. *Clinical Science* 96: 171-178

Bièche I, Olivi M, Champème M-H, Vidaud D, Lidereau R, and Vidaud M (1998). Novel approach to Quantitative Polymerase Chain Reaction using real-time detection: application to the detection of gene amplification in breast cancer. *Int J Cancer* 78: 661-666

Bohney JP, Fonda ML, and Feldhoff RC (1992). Identification of Lys190 as the primary binding site for pyridoxal 5'-phosphate in human serum albumin. *FEBS Lett* 298: 266-268

Buckingham M, and Rigby PWJ (2014). Gene regulatory networks and transcriptional mechanisms that control myogenesis. *Dev Cell* 28: 225-238

Di Salvo ML, Contestabile R, and Safo MK (2011). Vitamin B_6 salvage enzymes: Mechanism, structure and regulation. *Biochim Biophys Acta* 1814: 1597-1608

Dias B, and Weimer B (1998). Purification and functional analysis of L-Methionine-γ-lyase from *Brevibacterium linens* BL2. *Appl Env Microbiol* 64: 3327-3331

Ehrich M, Turner J, Gibbs P, Lipton L, Giovanetti M, Cantor C, and van den Boom D (2008). Cytosine methylation profiling of cancer cell lines. *Proc Natl Acad Sci USA* 105: 4844-4849

Forquin M-P, Hébert A, Roux A, Aubert J, Proux C, Heilier J-F, Landaud S, Junot C, Bonnarme P, and Martin-Verstraete I (2011). Global regulation of the response to sulfur availability in the cheese-related bacterium *Brevibacterium aurantiacum*. *Appl Env Microbiol* 77: 1449-1459

Gay F, Aguera K, Sénéchal K, Tainturier A, Berlier W, Maucort-Boulch D, Honnorat J, Horand F, Godfrin Y, and Bourgeaux V (2017). Methionine tumor starvation by erythrocyte-encapsulated methionine gamma-lyase activity controlled with per os vitamin B6. *Cancer Medicine* 6: 1437-1452

Goyer A, Collakova E, Shachar-Hill Y, and Hanson AD (2007). Functional Characterization of a Methionine γ-Lyase in Arabidopsis and its implication in an alternative to the reverse trans-sulfuration pathway *Plant Cell Physiol* 48: 232–242

Halpern BC, Clark BR, Hardy DN, Halpern RM and Smith RA (1974). The effect of replacement of methionine by homocystine on survival of malignant and normal adult mammalian cells in culture. *Proc Natl Acad Sci USA* 71: 1133-1136

Hanniffy SB, Philo M, Peláez C, Gasson MJ, Requena T, and Martínez-Cuesta MC (2009). Heterologous production of Methionine-γ-Lyase from *Brevibacterium linens* in *Lactococcus lactis* and formation of volatile sulfur compounds. *Appl Env Microbiol* 75: 2326-2332

Herman JG, Merlo A, Mao L, Lapidus RG, Issa J-PJ, Davidson NE, Sidransky D, and Baylin SB (1995). Inactivation of the CDKN2/p16/MTS1 gene is frequently associated with aberrant DNA methylation in all common human cancers. *Cancer Res* 55: 4525-4530

Hinshelwood RA, Melki JR, Huschtscha LI, Paul C, Song JZ, Stirzaker C, Reddel RR, and Clark SJ (2009). Aberrant de novo methylation of the $p16^{INK4A}$ CpG island is initiated post gene silencing in association with chromatin remodeling and mimics nucleosome positioning. *Hum Mol Genet* 18: 3098-3109

Hoffman RM, and Erbe RW (1976). High in vivo rates of methionine biosynthesis in transformed human and malignant cells auxotrophic for methionine. *Proc Natl Acad Sci USA* 73: 1523-1527

Hori H, Takabayashi K, Orvis L, Carson DA, and Nobori T (1996). Gene cloning and characterization of *Pseudomonas putida* L-Methionine-α-deamino-γ-mercaptoethane-lyase. *Cancer Res* 56: 2116-2121

Kokkinakis DM (2006). Methionine-stress: A pleiotropic approach in enhancing the efficacy of chemotherapy. *Cancer Lett* 233: 195-207

Kondo Y, Shen L, and Issa J-PJ (2003). Critical role of histone methylation in tumor suppressor gene silencing in colorectal cancer. *Mol Cell Biol* 23: 206-215

Kondo Y, Shen L, Yan PS, Huang TH-M, and Issa J-PJ (2004). Chromatin immunoprecipitation microarrays for identification of genes silenced by histone H3 lysine 9 methylation. *Proc Natl Acad Sci USA* 101: 7398–7403

Kudou D, Misaki S, Yamashita M, Tamura T, Esaki N, and Inagaki K (2007). Structure of the antitumour enzyme L-Methionine γ-lyase from *Pseudomonas putida* at 1.8 Å resolution. *J Biochem* 141: 535-544

Kudou D, Misaki S, Yamashita M, Tamura T, Esaki N, and Inagaki K (2008). The role of cysteine 116 in the active site of the antitumor enzyme L-methionine γ-lyase from *Pseudomonas putida*. *Biosci Biotechnol Biochem* 72: 1722-1730

Kulikova VV, Morozova EA, Revtovich SV, Kotlov MI, Anufrieva NV, Bazhulina NP, Raboni S, Faggiano S, Gabellieri E, Cioni P et al. (2017). Gene cloning, characterization, and cytotoxic activity of methionine γ-lyase from *Clostridium novyi*. *IUBMB Life* 69: 668-676

Li J, Poi M J, and Tsai M-D. The regulatory mechanisms of tumor suppressor $P16^{INK4A}$ and relevance to cancer (2011). *Biochemistry* 50: 5566-5582

Machover D, Goldschmidt E, Mollicone R, Haghighi-Rad F, Desterke C, Gaston-Mathé Y, Saffroy R, Boucheix C, and Dairou J (2018). Enhancement of 5-fluorouracil cytotoxicity by pyridoxal 5'-phosphate and folinic acid in tandem. *J Pharmacol Exp Ther* 366: 238-243

Machover D, Zittoun J, Broët P, Metzger G, Orrico M, Goldschmidt E, Schilf A, Tonetti C, Delmas-Marsalet B, Luccioni C, et al. (2001). Cytotoxic synergism of methioninase in combination with 5-fluorouracil and folinic acid. *Biochem Pharmacol* 61: 867-876

Machover D, Zittoun J, Saffroy R, Broët P, Giraudier S, Magnaldo T, Goldschmidt E, Debuire B, Orrico M, Tan Y, et al. (2002). Treatment of cancer cells with methioninase produces DNA hypomethylation and increases DNA synthesis. *Cancer Res* 62: 4685-4689

Maeda N, Takahashi K, Aono K, and Shiga T (1976). Effect of pyridoxal 5'-phosphate on the oxygen affinity of human erythrocytes. *Br J of Haematol* 34: 501-509

Magnani M, Rossi L, Bianchi M, Fornaini G, Benatti U, Guida L, Zocchi E, de Flora A (1988). Improved metabolic properties of hexokinase-overloaded human erythrocytes. *Biochim Biophys Acta* 972: 1-8

Meister A, and Anderson ME (1983). Glutathione. *Annu Rev Biochem* 52: 711-760

Sato D, and Nozaki T (2009). Methionine Gamma-Lyase: the unique reaction mechanism, physiological roles, and therapeutic applications against infectious diseases and cancers. *IUBMB Life* 61: 1019-1028

Stern PH, Wallace CD, and Hoffman RM (1984). Altered methionine metabolism occurs in all members of a set of diverse human tumor cells. *J Cell Physiol* 119: 29-34

Steele L, Mayer L, and Berin MC (2012). Mucosal immunology of tolerance and allergy in the gastrointestinal tract. *Immunol Res* 54: 75-82

Stone E, Paley O, Hu J, Ekerdt B, Cheung N-K, and Georgiou G (2012). De novo engineering of a human cystathionine-γ-lyase for systemic L-methionine depletion cancer therapy. *ACS Chem Biol* 7: 1822-1829

Sun X, Yang Z, Li S, Tan Y, Zhang N, Wang X, Yagi S, Yoshioka T, Takimoto A, Mitsushima K et al. (2003). In vivo efficacy of recombinant methioninase is enhanced by the combination of polyethylene glycol conjugation and pyridoxal 5′-phosphate supplementation. *Cancer Res* 63: 8377-8383

Takakura T, Mitsushima K, Yagi S, Inagaki K, Tanaka H, Esaki N, Soda K, and Takimoto A (2004). Assay method for antitumor L-Methionine γ-lyase: comprehensive kinetic analysis of the complex reaction with L-methionine. *Anal Biochem* 327: 233-240

Tokoro M, Asai T, Kobayashi S, Takeuchi T, and Nozaki T (2003). Identification and characterization of two isoenzymes of Methionine γ-lyase from *Entamoeba histolytica*. *J Biol Chem* 278: 42717-42727

Watervall WA, Scheijen JLJM, Ortmans-Ploemen MMJC, Habets-van der Poel CD, and Bierau J (2009). Quantitative UPLC-MS/MS analysis of underivatised amino acids in body fluids is a reliable tool for the diagnosis and follow-up of patients with inborn errors of metabolism. *Clin Chim Acta* 407: 36-42

Yang Z, Sun X, Li S, Tan Y, Wang X, Zhang N, Yagi S, Takakura T, Kobayashi Y, Takimoto A et al. (2004). Circulating half-life of PEGylated recombinant methioninase holoenzyme is highly dose dependent on cofactor Pyridoxal-5'-phosphate. *Cancer Res* 64: 5775-5778

Yoshioka T, Wada T, Uchida N, Maki H, Yoshida H, Ide N, Kasai H, Hojo K, Shono K, Maekawa R et al. (1998). Anticancer efficacy in vivo and in vitro, synergy with 5-fluorouracil, and safety of recombinant methioninase. *Cancer Res* 58: 2583-2587

Zempleni J, and Kübler W (1994). The utilization of intravenously infused pyridoxine in humans. *Clinical Chimica Acta* 229: 27-36.

Footnotes

Support: The present work was supported by the Institut du Cancer et d'Immunogénétique (ICIG), Hospital Paul-Brousse, 94800 Villejuif, France.

Authorizations: Murine experiments were performed under authorization No 94-323 to INSERM, Hospital Paul-Brousse and University Paris XI, Villejuif, France, issued from the Veterinary Services from Val-de-Marne, France. Human blood for encapsulation experiments was obtained from adult volunteers under protocol No 6589 approved by the Ethics Committee of the University of Urbino *Carlo Bo*.

Potential conflict of interest disclosure statement: David Machover and Pascal Bonnarme are co-authors of the United States patent No. 9,051,562 B2 dated June 9, 2015, entitled *Polypeptides isolated from Brevibacterium aurantiacum and their use for the treatment of cancer*. Assignees: Institut National de la Santé et de la Recherche Médicale (INSERM); Institut National de la Recherche Agronomique (INRA); and Université Paris Sud-Paris XI.

Legends for Figures

Figure 1. Enzymatic activity of native MGL-BL929 incubated for 8 hours (A), and 24 hours (B) was assayed at 37°C under four different conditions. Conditions were (I) phosphate-buffered saline (PBS); (II) PBS supplemented with human serum albumin at 40 g/L; (III) pure human plasma, and (IV) pure rat plasma. Measurement of enzyme activity was performed without additional PLP, and under three PLP concentrations (*i.e.*, 20 μM, 100 μM, and 200 μM). Bars are the mean of experiments done in quadruplicate ± SE. Analysis of variance found significant differences between incubation conditions at 8 hours (***$P = 2.2\text{x}10^{-16}$), and at 24 hours (***$P = 2.75\text{x}10^{-7}$), and between PLP concentrations at 8 hours (***$P = 8.8\text{x}10^{-5}$).

Figure 2. L-Methionine concentration changes in supernatant of HT29, SKOV3, JURKAT, and REH cells growing in standard cell culture media (*i.e.*, RPMI 1640, or DMEM) supplemented with 10% FBS, exposed to various concentrations of MGL-BL929 for 24h, 48h, 72h, and 96h. L-Met elimination rates were the ratios of the concentrations measured in supernatant of cells exposed to MGL-BL929 over that found in cells unexposed to the enzyme at same time to take account of consumption of L-methionine by growing cancer cells. RPMI 1640, and DMEM media contain L-Methionine at 100 μM, and 200 μM, respectively.

Figure 3. Mean methyl-CpG percent change from control of gene promoters in colorectal cancer HT29 cells exposed to MGL-BL929 at 2 Unit/ml for 72 hours. Methylation rates in fragments with a single CpG or groups of 2 to 5 contiguous CpGs were measured in 84 DNA fragments comprising 131 CpG dinucleotides whose baseline methyl-CpG levels in control cells were greater than 70% (mean percent methyl-CpG, 88.67). Bars represent the difference in mean methyl-CpG level of fragments in cells exposed to the MGL-BL929 and that in control cells unexposed to the enzyme. Numbers under bars indicate positions from the first nucleotide of coding DNA sequences to each single 5-meC or groups of 5-meCs within CpG dinucleotides of gene promoters. The difference between percent methylation in paired samples was statistically significant (Two-sided Wilcoxon Rank-Sum Test, ***$P = 6.5\text{x}10^{-5}$). Methyl CpG change in cells exposed to MGL-BL929 at 1 Unit/ml for 72 hours is shown in Supplemental Figure S1.

Figure 4. CDKN2A gene expression changes by quantitative RT-PCR in HT29 (A) and in HCT116 (B) colorectal carcinoma cell lines exposed to MGL-BL929 at 1 Unit/ml and 2 Unit/ml for 48h and 72h. CDKN2A mRNA expression was normalized using 18S-rRNA as reference gene. The amount of cDNA from CDKN2A gene was divided by that of 18S-rRNA gene under each condition to obtain a normalized ratio value. Relative expression level was obtained by dividing normalized ratio values obtained with cells exposed to the MGL-BL929 under each condition by the normalized ratio in control cells unexposed to the enzyme at same time point. Bars indicate N-fold change ± SE.

Figure 5. Western blots of $p16^{INK4A}$ in HT29, HCT116 colon carcinoma, and in HeLa cervix adenocarcinoma cells exposed to MGL-BL929 at 1 Unit/ml during 48 hours. Figure represents two separate experiments. *Experiment 1*: Lanes 1 and 3 represent blots from cells unexposed and exposed to the enzyme, respectively; and *Experiment 2*: Lanes 2 and 4 represent blots from cells unexposed and exposed to the enzyme, respectively. The protein $p16^{INK4A}$ was not detected in colon carcinoma cell lines, but was expressed in HeLa cells. No appreciable change in band intensities was observed according to experimental condition in each experiment. Antibodies against $p16^{INKA}$ were 108349 (Abcam), and 1D7D2 (ThermoFisher).

Figure 6. Western blots of global histone H3 dimethyl-lysine9 (H3K9me2) and of total Histone H3 in HT29 and HCT116 cells exposed to MGL-BL929 at 1 Unit/ml or 2 Unit/ml for 48 hours and 72 hours. Decrease in band intensities of global H3K9me2 ranging from 77% to 89% (mean decrease, 83%) from that in control occurred in HT29 and HCT116 cells exposed to MGL-BL929 at 1 Unit/ml and 2 Unit/ml, except for one single smaller decrease by 38% in HT29 cells exposed to the enzyme at 1 Unit/ml for 72 hours. Relative band intensity changes by ± 15% were not observed in total histone H3, and in H3K4me2, H3K27me2, H3K36me2, and H3K79me2.

Figure 7. L-Methionine γ-lyase activity in human erythrocytes encapsulated with MGL-BL929. Cells were incubated at 0.5% erythrocyte volume fraction in 50 mM NaH_2PO_4/Na_2HPO_4, 90 mM NaCl, 5 mM glucose, 200 μM PLP, and 100 μM L-methionine; pH 7.4 at 37°C in an atmosphere containing 5% CO_2. Enzyme activity was assayed at t_0, and then every 24 hours during 96 hours. Erythrocytes were loaded with encapsulation solution containing the enzyme at 270 Unit/ml (circles), 54 Unit/ml (squares), or 11 Unit/ml (triangles). Values (in Unit/ml of packed cells) represent mean activity ± SE. The inset represents estimation of MGL-BL929 load in erythrocytes by Western blot at t_0 in cells subjected to encapsulation in the presence of various concentrations of the enzyme; concentrations of MGL-BL929 in encapsulation solution (Unit/ml) were: 45 (lane 1); 90 (lane 2); 180 (lane 3); and 270 (lanes 4 and 6). Lane 5 was obtained from unloaded (UL) cells (*i.e.*, cells that were subjected to the loading procedure without the enzyme).

Figure 8. L-Methionine elimination from medium by human erythrocytes loaded with various amounts of MGL-BL929. Concentrations of enzyme in encapsulation solution were 270 Unit/ml (A), 54 Unit/ml (B), or 11 Unit/ml (C). Elimination of L-methionine was assessed in supernatant of MGL-BL929-loaded erythrocytes incubated at 0.5% cell volume fraction in 50 mM NaH_2PO_4/Na_2HPO_4, 90 mM NaCl, 5 mM glucose, 200 μM PLP, and 100 μM L-methionine; pH 7.4 at 37°C in an atmosphere containing 5% CO_2. Measurements of L-methionine were done at t_0, and then every 24 hours during four days. Bars indicate mean values of ≥ 2 experiments ± SE.

Figure 9. Elimination of L-methionine in supernatant of MGL-BL929-loaded human erythrocytes incubated at 0.5% cell volume fraction at 37°C in an atmosphere containing 5% CO_2 in media containing various B6 vitamers. Media consisted of 50 mM NaH_2PO_4/Na_2HPO_4, 90 mM NaCl, 5 mM glucose, and 100 μM L-methionine; pH 7.4, supplemented with vitamin B6 in the form of (A) PLP at 200 μM, (B) PLP at 0.1 μM, (C) pyridoxine (PN) at 200 μM, or (D) pyridoxamine (PM) at 200 μM. Erythrocytes were loaded with MGL-BL929 at 54 U/ml in encapsulation solution. Measurements were done at t_0, and then at various times up to 120 hours (inset) from loading. Concentrations of L-methionine after 120 hours of incubation (*d* columns) were ≤ 3 μM in all conditions.

Figure 10. Elimination of high-concentration L-Methionine from medium by MGL-BL929-encapsulated human erythrocytes. Cells were loaded with the enzyme at 270 Unit/ml in encapsulation solution. Elimination of L-methionine was assessed in supernatant of MGL-BL929-loaded erythrocytes incubated at 0.5% cell volume fraction at 37°C in an atmosphere containing 5% CO_2 in media consisting of 50 mM NaH_2PO_4/Na_2HPO_4, 90 mM NaCl, 5 mM glucose, and 200 μM PLP; pH 7.4, supplemented with 1 mM L-methionine once at t_0 (I), twice at t_0, and t_{24h} (II), and three times at t_0, t_{24h}, and t_{48h} (III). Measurements were done at t_0, and then every 24 hours from loading up to 96 hours. Comparisons of residual L-methionine from days 1 to 4 by analysis of variance did not find any significant difference between experimental conditions I, II, and III ($P = 0.12$), and between days of incubation ($P = 0.36$). Bars represent mean values from experiments done in duplicate ± SE.

JPET Fast Forward. Published on April 2, 2019 as DOI: 10.1124/jpet.119.256537
This article has not been copyedited and formatted. The final version may differ from this version.

Table 1. DNA sequences of the L-Methionine γ-Lyase BL-929 and sequence of the protein

Sequence 1

>DNA sequence from *Brevibacterium aurantiacum*

ATGACCTCACTGCACCCAGAAACGCTCATGGTCCACGGCGGAATGAAAGGCCTCACCGAG
GCAGGAGTCCACGTACCGGCCATCGACCTCTCGACCACCAACCCAGTCAACGATGTCGCC
ACCGGCGGTGACTCCTACGAATGGCTCGCCACCGGCCATACGCTCAAGGACGGCGACTCG
GCCGTCTACCAGCGCCTCTGGCAGCCCGGTGTCGCACGCTTCGAGACCGCGCTGGCCGGG
CTCGAACACGCTGAGGAAGCAGTCGCCTTCGCCACGGGCATGGCCGCAATGACTGCCGCA
CTTCTCGCGGCCGTCAGCGCAGGAACACCCCACATCGTCGCAGTGCGTCCCCTCTATGGC
GGAAGCGACCACCTCCTCGAAACCGGACTGCTGGGGACAACAGTCACATGGGCAAAGGAA
GCCGACATCGCCTCGGCGATCCAAGATGACACCGGACTCGTCATTGTCGAGACCCCGGCA
AACCCCAGCCTGGACCTTGTTGATCTCGACAGTGTCGTCTCAGCCGCCGGCAACGTGCCT
GTGCTGGTGGACAACACATTCTGCACACCTGTTCTCCAGCAGCCCATCTCCCACGGAGCG
GCCCTCGTACTGCACAGCGCGACAAAATACCTCGGCGGTCATGGCGATGCCATGGGCGGC
ATCATCGCCACCAACGCCGACTGGGCGATGCGCCTGCGACAGGTCCGAGCCATCACAGGA
GCCCTGCTCCACCCCATGGGCGCGTATCTCCTTCATCGGGGCTTGCGCACTCTGGCCGTG
CGCATGCGCGCGGCTCAGACCACCGCCGGTGAGCTCGCTGAGCGCCTGGACGCGCACCCT
GCCATCTCCGTCGTCCACTACCCGGGACTGAAAGGCCAGGACCCACGCGGACTGCTCGGA
CGCCAAATGTCCGGTGGTGGTGCGATGATCGCGATGGAGCTCGCCGGTGGATTCGACGCC
GCCCGCAGCTTCGTCGAACACTGCAACCTCGTCGTCCACGCGGTGTCCCTGGGCGGCGCT
GACACTCTCATCCAGCATCCGGCGTCACTGACTCACAGGCCAGTTGCGGCCACGGCGAAG
CCCGGCGATGGTCTCATCCGACTCTCTGTGGGACTCGAACACGTCGATGACCTGGCAGAC
GATCTCATCGCTGCCCTCGACGCGAGTCGGGCCGCTGCCTGA

Sequence 2

>Sequence of translated protein

MTSLHPETLMVHGGMKGLTEAGVHVPAIDLSTTNPVNDVATGGDSYEWLATGHTLKDGDS
AVYQRLWQPGVARFETALAGLEHAEEAVAFATGMAAMTAALLAAVSAGTPHIVAVRPLYG
GSDHLLETGLLGTTVTWAKEADIASAIQDDTGLVIVETPANPSLDLVDLDSVVSAAGNVP
VLVDNTFCTPVLQQPISHGAALVLHSATKYLGGHGDAMGGIIATNADWAMRLRQVRAITG
ALLHPMGAYLLHRGLRTLAVRMRAAQTTAGELAERLDAHPAISVVHYPGLKGQDPRGLLG
RQMSGGGAMIAMELAGGFDAARSFVEHCNLVVHAVSLGGADTLIQHPASLTHRPVAATAK
PGDGLIRLSVGLEHVDDLADDLIAALDASRAAA

Sequence 3

>DNA sequence optimized for *E. coli* expression

ATGACCTCGCTGCATCCCGAGACGCTGATGGTTCATGGTGGAATGAAGGGTCTGACCGAA
GCTGGAGTTCATGTCCCGGCAATTGATCTGAGCACCACCAATCCCGTCAATGATGTCGCA
ACCGGTGGAGATTCCTATGAGTGGCTGGCCACCGGTCATACGCTGAAAGATGGTGATAGC
GCAGTTTATCAGCGTCTGTGGCAGCCTGGGGTTGCTCGTTTTGAAACCGCTCTGGCAGGG
CTGGAGCATGCTGAAGAGGCTGTTGCATTTGCAACGGGTATGGCAGCTATGACTGCAGCT
CTACTGGCTGCAGTTTCAGCTGGAACACCCCACATTGTTGCTGTAAGACCTCTGTACGGT
GGAAGCGACCATCTGCTGGAGACCGGACTGCTGGGAACTACGGTTACTTGGGCTAAAGAG
GCAGATATTGCAAGCGCTATTCAAGACGATACCGGACTGGTTATAGTTGAAACCCCGGCT
AATCCTTCACTGGATCTAGTCGACCTGGATTCGGTTGTTTCGGCAGCAGGTAATGTACCC
GTCCTGGTCGATAATACTTTTTGTACTCCCGTCCTGCAGCAGCCTATTTCCCATGGAGCT
GCACTGGTCCTGCATTCTGCTACTAAGTATCTGGGTGGGCACGGTGACGCAATGGGTGGT
ATTATTGCAACCAATGCAGATTGGGCTATGCGTCTGAGACAGGTTAGAGCAATTACCGGA
GCACTGCTGCATCCTATGGGTGCTTACCTGCTACATCGGGGTCTCCGTACTCTGGCAGTA
CGTATGCGTGCTGCTCAGACCACCGCAGGGGAACTGGCTGAACGTCTGGATGCTCATCCC
GCAATTTCCGTTGTTCATTATCCGGGACTGAAGGGTCAGGATCCCCGTGGACTGCTGGGA
CGTCAAATGTCCGGGGGGGGGGCGATGATTGCTATGGAACTGGCAGGGGGCTTTGATGCA
GCACGTAGTTTTGTTGAGCATTGTAATCTGGTTGTTCATGCTGTATCCCTGGGTGGTGCT
GATACTCTGATTCAGCACCCGGCTTCGCTGACTCATAGGCCCGTCGCGGCCACGGCGAAA
CCTGGTGACGGGCTGATTAGACTGTCGGTAGGACTGGAGCATGTTGACGATCTGGCTGAT
GACCTGATTGCTGCACTGGATGCTTCGCGGGCAGCTGCATAA

Table 2. Cytotoxicity of MGL-BL929 in human cells

Cancer cell line	Tumor type	IC_{50} of MGL-BL929 in Unit/ml (95% CI)
HCT116	Colorectal carcinoma	0.18 (0.13-0.25)
HT29	Colorectal carcinoma	0.56 (0.49-0.64)
LoVo	Colorectal carcinoma	1.32 (1.22-1.42)
SW480[1]	Colorectal carcinoma	>3.5
SW620[1]	Colorectal carcinoma	>3.5
HeLa	Cervix adenocarcinoma	0.76 (0.46-1.26)
A431	Vulvar epidermoid carcinoma	0.84 (0.58-1.20)
HUH7	Hepatocellular carcinoma	1.84 (1.77-1.93)
MAHLAVU	Hepatocellular carcinoma	1.78 (1.67-1.89)
HepG2	Hepatoblastoma	0.78 (0.61-0.99)
HOON	Pre B-cell acute lymphocytic leukemia	0.29 (0.19-0.46)
REH	Pre-B cell acute lymphocytic leukemia	0.05 (0.02-0.14)
JURKAT	T-Cell acute lymphocytic leukemia	0.16 (0.07-0.37)
K562	CML blast crisis	0.20 (0.13-0.30)
HEL	Erythroleukemia	0.15 (0.08-0.27)
HL-60	Acute promyelocytic leukemia	0.08 (0.04-0.16)
KG-1	Acute myelocytic leukemia	0.48 (0.29-0.79)
BJAB	Burkitt's lymphoma	0.35 (0.31-0.40)
RAJI	Burkitt's lymphoma	0.18 (0.12-0.28)
U-2 OS	Osteosarcoma	0.59 (0.45-0.76)
HT-1080	Fibrosarcoma	0.64 (0.57-0.72)
PC-3	Prostate adenocarcinoma	0.80 (0.77-0.84)
OVCAR3	Ovarian adenocarcinoma	0.74 (0.53-1.05)
SKOV3	Ovarian adenocarcinoma	1.26 (1.06-1.51)
AsPC1	Pancreas adenocarcinoma	0.17 (0.09-0.35)
MCF7	Mammary adenocarcinoma	0.58 (0.23-1.43)
MDA-MB231	Mammary adenocarcinoma	0.61 (0.58-0.65)
SKBR3	Mammary adenocarcinoma	1.87 (1.41-2.48)
A375	Melanoma	0.39 (0.31-0.48)
SKMEL28	Melanoma	1.31 (1.04-1.65)
RCC7	Renal cell carcinoma	0.94 (0.74-1.19)
A-549	Lung adenocarcinoma	1.17 (0.95-1.45)
H1993	Lung adenocarcinoma	2.14 (1.89-2.43)
IMR32	Neuroblastoma	0.24 (0.10-0.54)
HTB-14	Glioma	1.56 (1.08-2.26)
Non-cancer cell	Cell type	IC_{50} of MGL-BL929 in Unit/ml
533[2]	Skin fibroblast	4.7
CDG-II[3]	Skin fibroblast	>10

[1]SW480 and SW620 colorectal cancer cells originate respectively from the primary tumor and a metastatic site from a single individual. [2]Primary 533 skin fibroblasts originated from a normal child, and [3]CDG-II cells were from an individual with Congenital Disorder of Glycosylation II. Cells were counted after 72-hour exposure to MGL-BL929. Dose-effect plots were obtained with the CalcuSyn v2 software.

Table 3. Enzyme kinetics of MGL-BL929 with sulfur-containing amino acids and substituted amino acids

Amino acid and substituted amino acid	K_M (mM)	k_{cat} (s^{-1})	Specific activity (μmol mn^{-1} mg^{-1})
L-Methionine	6.83 ± 2.45	15.51 ± 3.23	5.77 ± 1.4
L-Homocysteine	0.94 ± 0.8	72.44 ± 12.38	27.7 ± 5.7
L-Cysteine	-	-	Nd
L-Cystathionine	-	-	Nd
S-Adenosyl-L-homocysteine	-	-	Nd
D-Methionine	-	-	Nd

Values are mean ± SE from two to 4 separate experiments with each amino acid or substituted amino acid

One unit of enzyme is defined as the amount that catalyzes formation of 1 μmol of α-ketobutyrate per minute from L-methionine

Nd: no detectable activity.

JPET Fast Forward. Published on April 2, 2019 as DOI: 10.1124/jpet.119.256537
This article has not been copyedited and formatted. The final version may differ from this version.

Table 4. Changes in gene promoter CpG methylation in HT29 cells exposed to MGL-BL929

MGL-BL929 (Unit/ml)	Mean percent 5-methyl-CpG[1] and mean difference from control[2] at		
	24 hours	48 hours	72 hours
1 Unit/ml[2,3,5]	$Enz_{control}$ 89.1	$Enz_{control}$ 89.21	$Enz_{control}$ 88.64
	$Enz_{1Unit/ml}$ 89.68	$Enz_{1Unit/ml}$ 86.35	$Enz_{1Unit/ml}$ 81.84
	Δ $Enz_{control}$:$Enz_{1Unit/ml}$ 0.58	Δ $Enz_{control}$:$Enz_{1Unit/ml}$ -2.86	Δ $Enz_{control}$:$Enz_{1Unit/ml}$ -6.8
	$P = 0.52$ (NS)	$^{**}P = 5.7\text{x}10^{-3}$	$^{***}P = 1.3\text{x}10^{-9}$
2 Unit/ml[2,4,5]	$Enz_{control}$ 89.16	$Enz_{control}$ 91.22	$Enz_{control}$ 88.67
	$Enz_{2Unit/ml}$ 88.54	$Enz_{2Unit/ml}$ 85.7	$Enz_{2Unit/ml}$ 82.9
	Δ $Enz_{control}$:$Enz_{2Unit/ml}$ -0.61	Δ $Enz_{control}$:$Enz_{2Unit/ml}$ -5.52	Δ $Enz_{control}$:$Enz_{2Unit/ml}$ -5.77
	$P = 0.63$ (NS)	$^{***}P = 4.1\text{x}10^{-6}$	$^{***}P = 6.5\text{x}10^{-5}$

[1]Methyl-CpG level under each experimental condition is the mean percent methylation of fragments from selected gene promoters comprising a single CpG or groups of 2 to 5 contiguous CpGs

[2]Changes of 5-methylcytosine (5-meC) levels within CpG dinucleotide in fragments from selected gene promoters containing 5-meC baseline levels greater than 70 % were studied in cells exposed to MGL-BL929 at 1 Unit/ml, and at 2 Unit/ml for 24h, 48h, and 72h. Results were expressed in percent methyl-CpG change between control cells unexposed to the enzyme and cells exposed to each concentration of MGL-BL929 at same times of growth. Mean percent methyl-CpG ± SE of gene promoter fragments from untreated cells was 89.25 ± 7.9.

[3]For cells exposed to MGL-BL929 at 1 Unit/ml, 142 fragments (including 230 CpGs), 141 fragments (including 228 CpGs), and 142 fragments (including 229 CpGs) were analysed after 24h, 48h, and 72h of exposure, respectively

[4]For cells exposed to MGL-BL929 at 2 Unit/ml, 91 fragments (including 146 CpGs), 81 fragments (including 129 CpGs), and 84 fragments (including 131 CpGs) were analysed after of 24h, 48h, and 72h of exposure, respectively

[5]Statistical comparisons of the difference between percent methylation in paired samples were done with two-sided Wilcoxon Rank-Sum Test. One-way ANOVA found significant differences in methylation rates according to time of enzyme exposure in cells exposed to MGL-BL929 at 1 Unit/ml ($^{***}P = 2\text{x}10^{-10}$) and 2 Unit/ml ($^{***}P = 5\text{x}10^{-5}$).

JPET Fast Forward. Published on April 2, 2019 as DOI: 10.1124/jpet.119.256537
This article has not been copyedited and formatted. The final version may differ from this version.

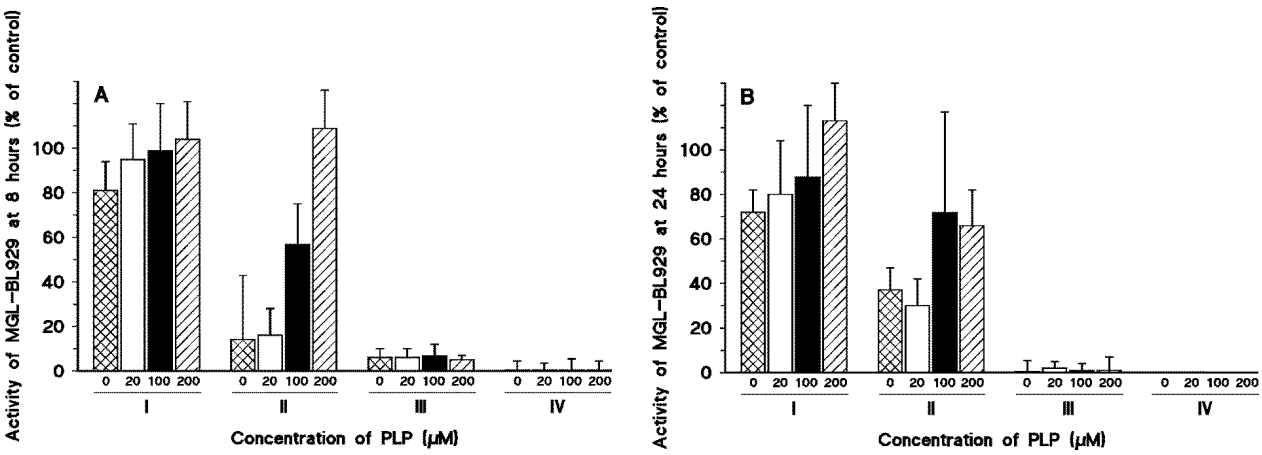

Figure 1.

JPET Fast Forward. Published on April 2, 2019 as DOI: 10.1124/jpet.119.256537
This article has not been copyedited and formatted. The final version may differ from this version.

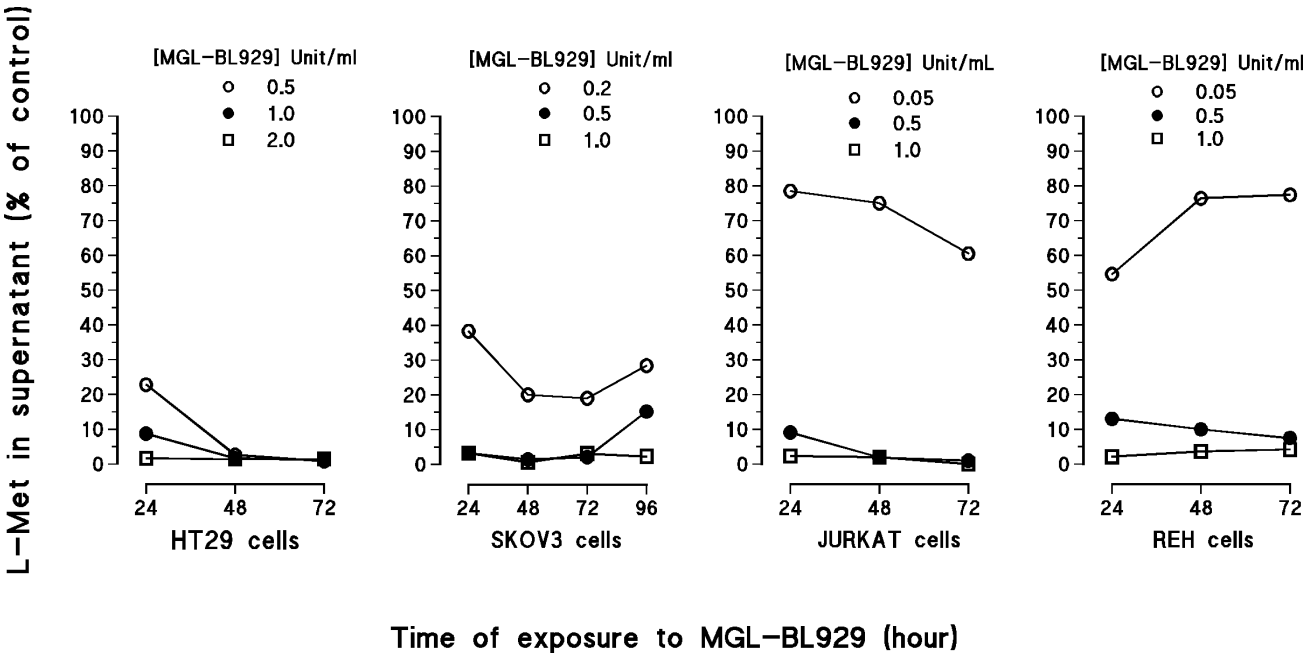

Figure 2.

JPET Fast Forward. Published on April 2, 2019 as DOI: 10.1124/jpet.119.256537
This article has not been copyedited and formatted. The final version may differ from this version.

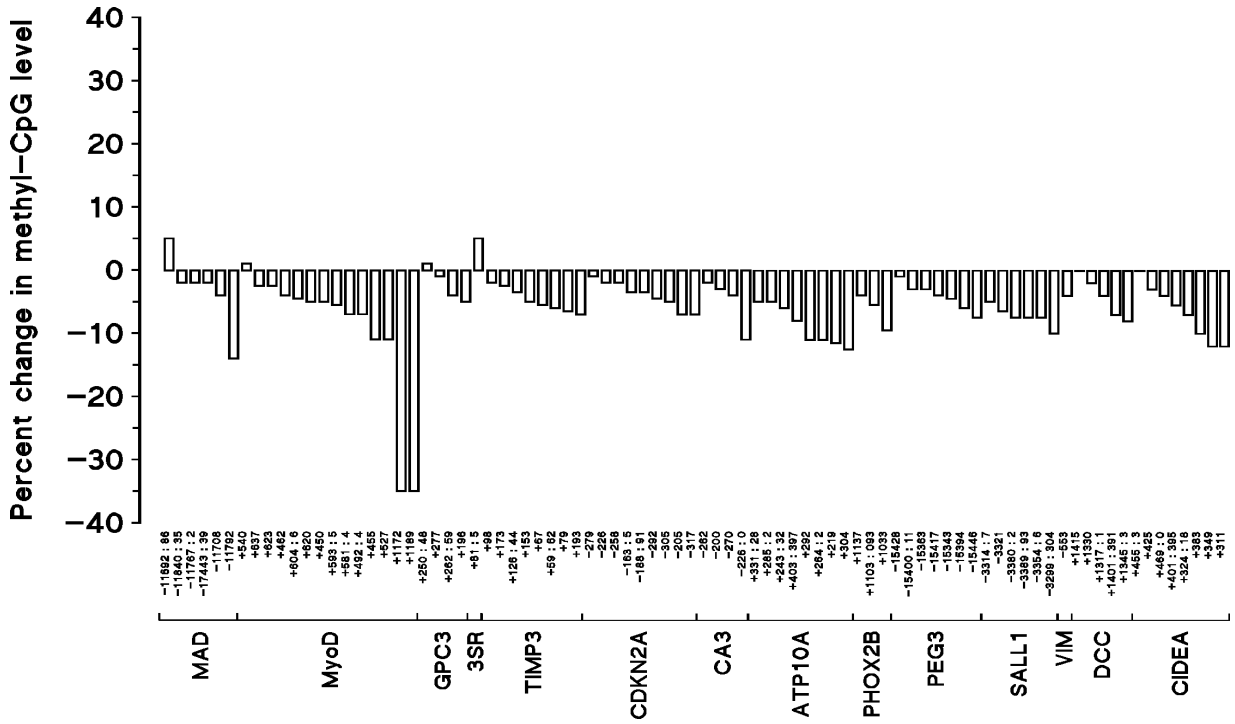

Figure 3.

JPET Fast Forward. Published on April 2, 2019 as DOI: 10.1124/jpet.119.256537
This article has not been copyedited and formatted. The final version may differ from this version.

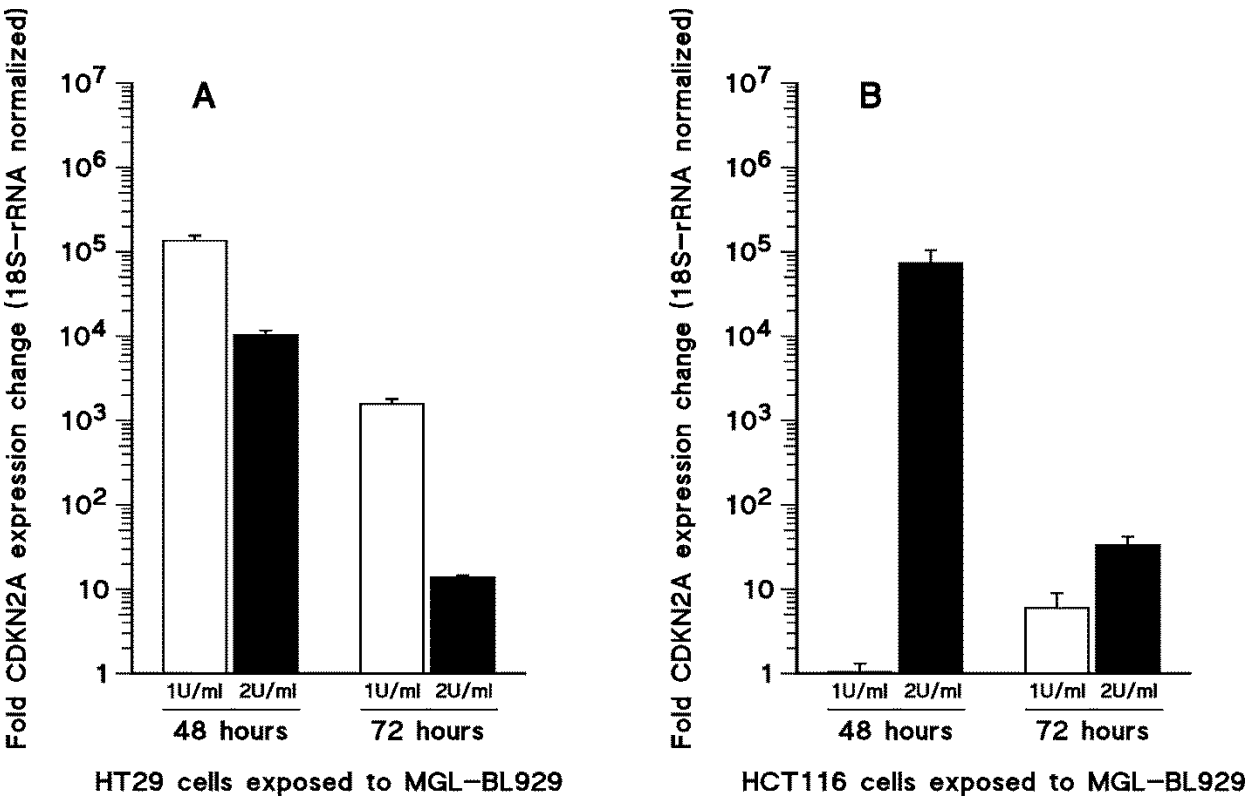

Figure 4.

JPET Fast Forward. Published on April 2, 2019 as DOI: 10.1124/jpet.119.256537
This article has not been copyedited and formatted. The final version may differ from this version.

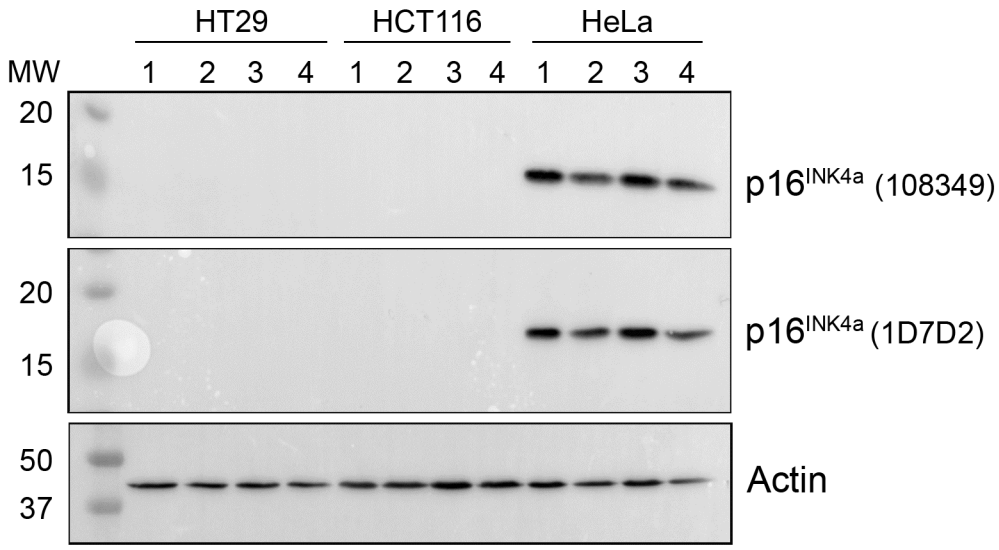

Figure 5.

JPET Fast Forward. Published on April 2, 2019 as DOI: 10.1124/jpet.119.256537
This article has not been copyedited and formatted. The final version may differ from this version.

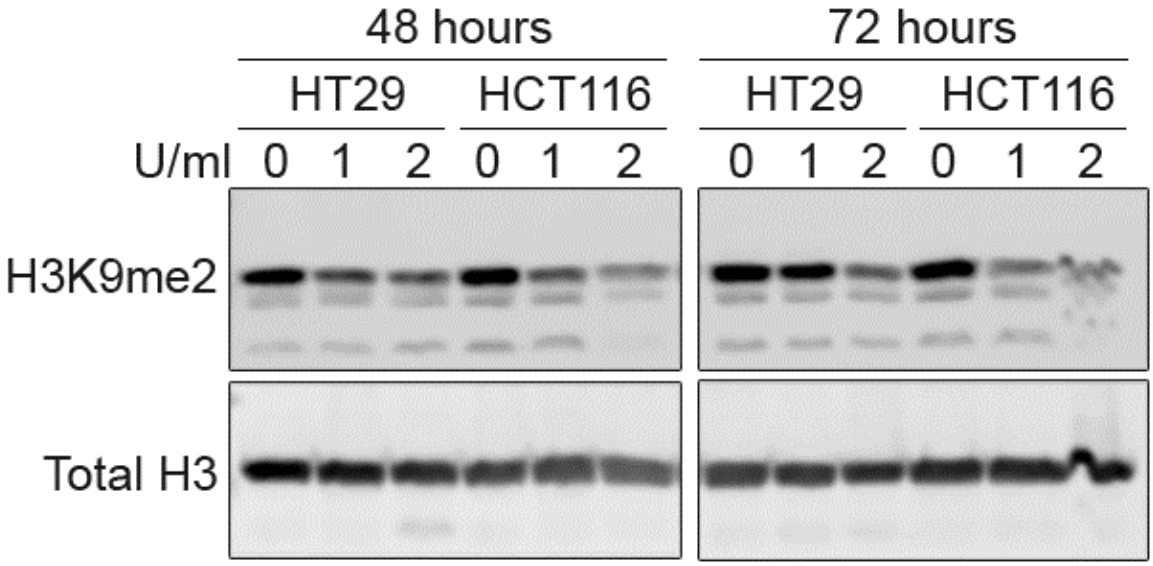

Figure 6.

JPET Fast Forward. Published on April 2, 2019 as DOI: 10.1124/jpet.119.256537
This article has not been copyedited and formatted. The final version may differ from this version.

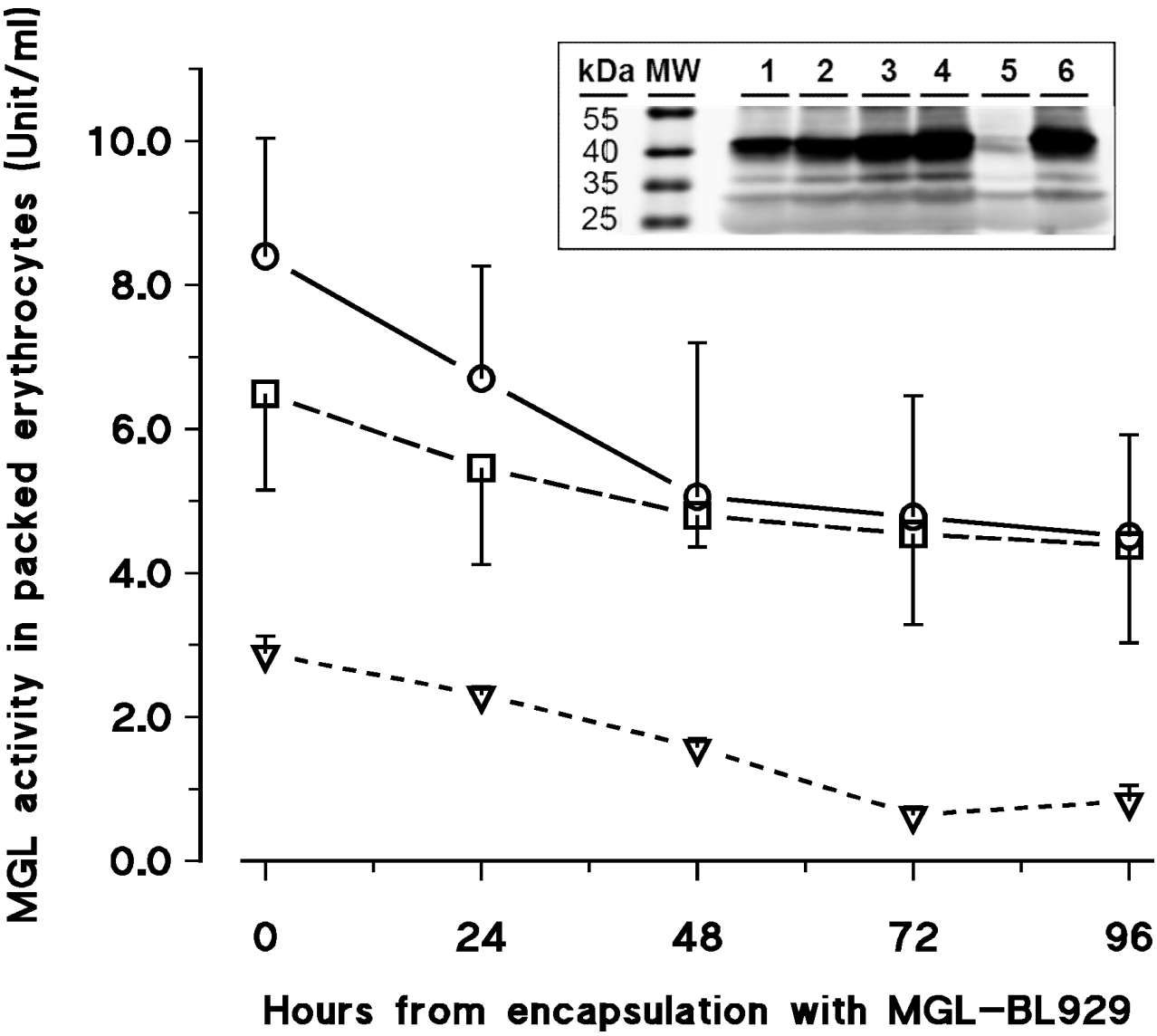

Figure 7.

JPET Fast Forward. Published on April 2, 2019 as DOI: 10.1124/jpet.119.256537
This article has not been copyedited and formatted. The final version may differ from this version.

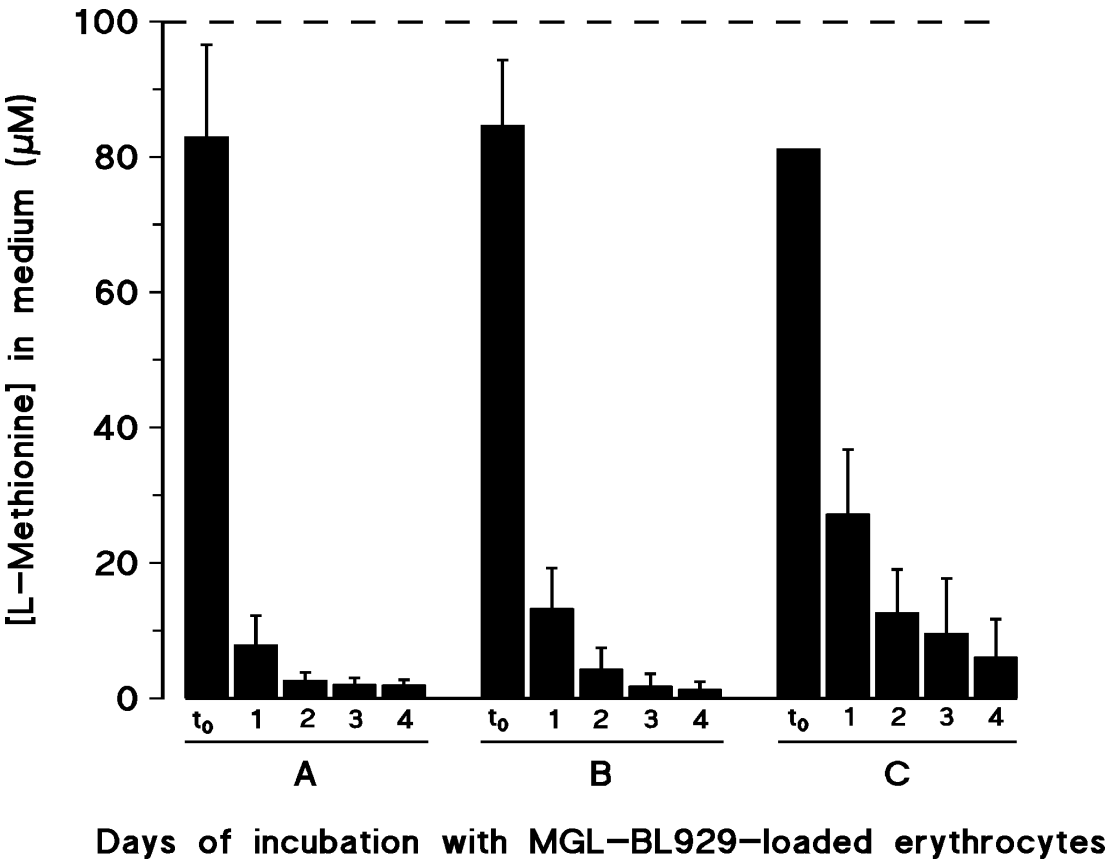

Figure 8.

JPET Fast Forward. Published on April 2, 2019 as DOI: 10.1124/jpet.119.256537
This article has not been copyedited and formatted. The final version may differ from this version.

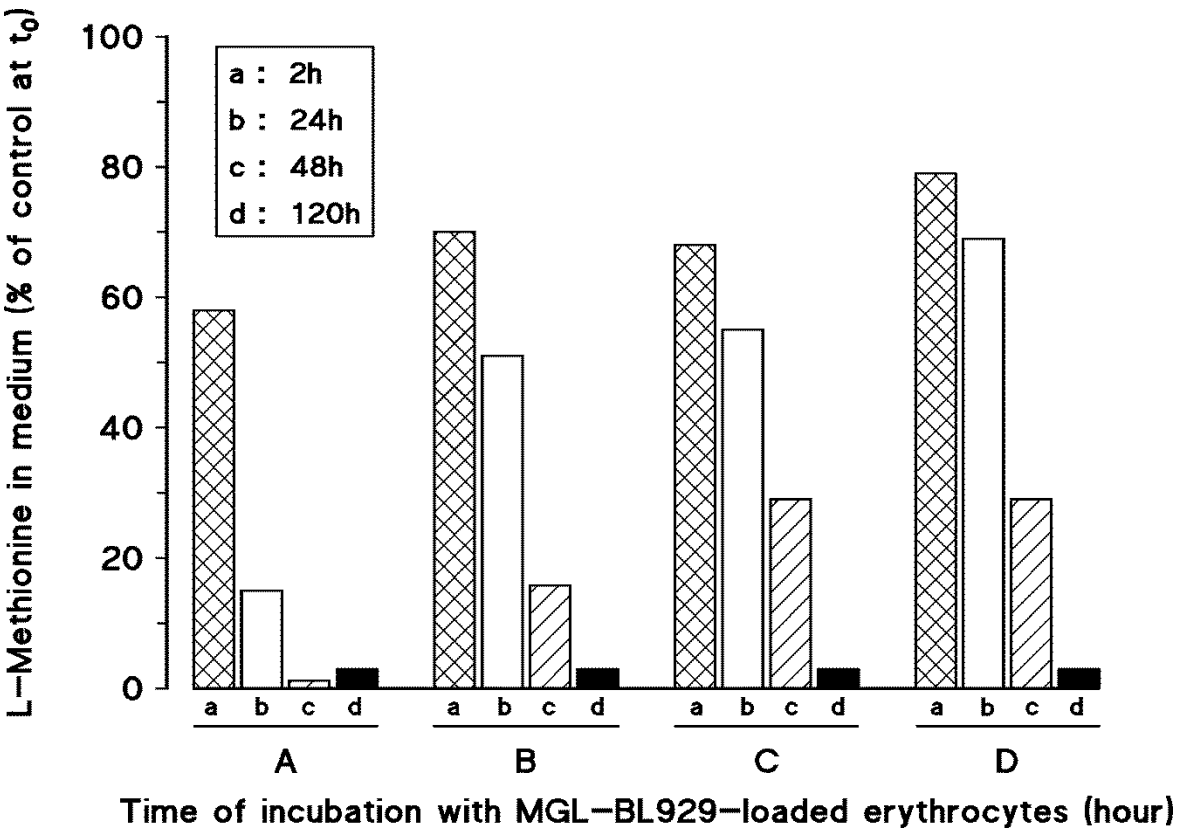

Figure 9.

JPET Fast Forward. Published on April 2, 2019 as DOI: 10.1124/jpet.119.256537
This article has not been copyedited and formatted. The final version may differ from this version.

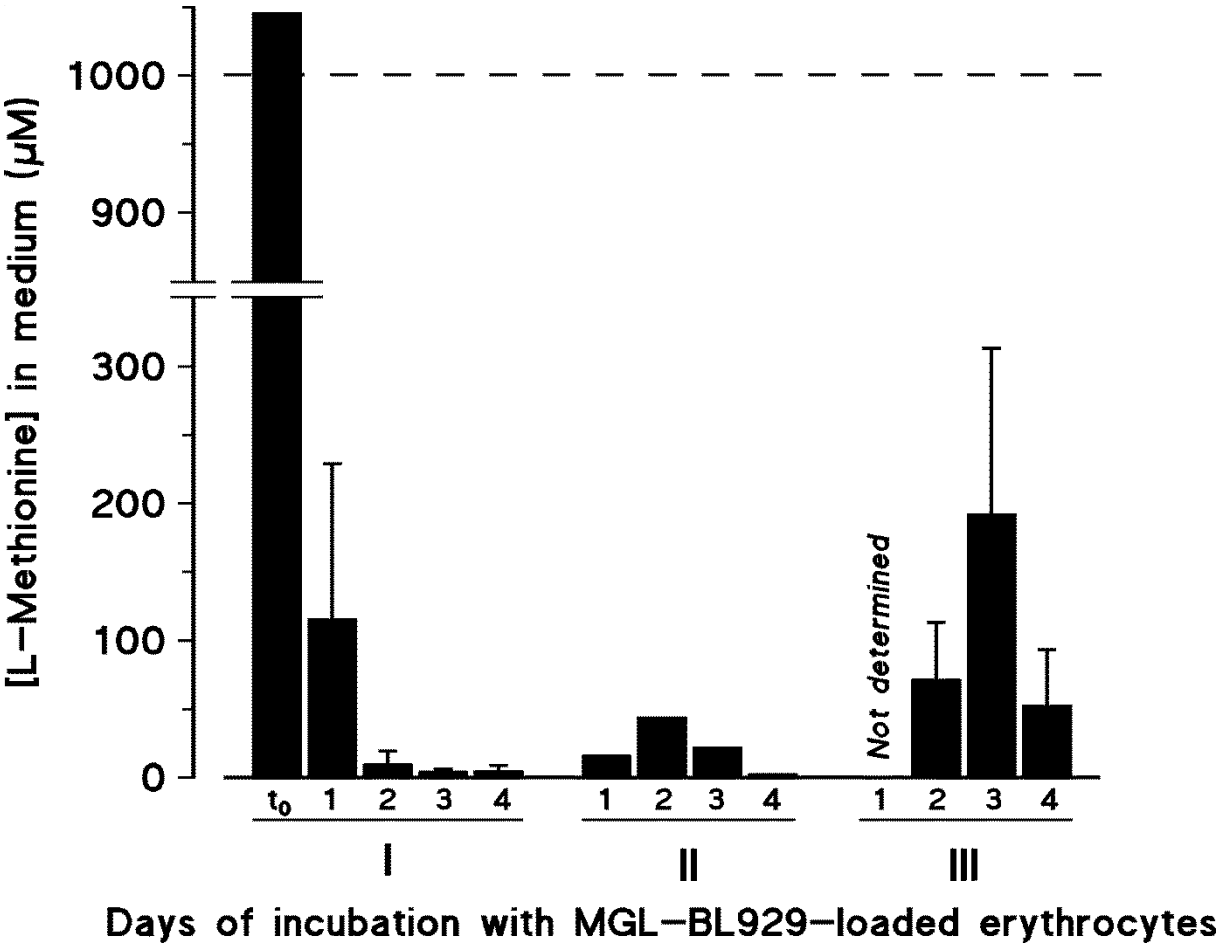

Figure 10.

Supplemental data

Effects in cancer cells of the recombinant L-Methionine gamma-lyase from *Brevibacterium aurantiacum.* Encapsulation in human erythrocytes for sustained L-methionine elimination

David Machover, Luigia Rossi, Jocelyne Hamelin, Christophe Desterke, Emma Goldschmidt, Bernadette Chadefaux-Vekemans, Pascal Bonnarme, Pierre Briozzo, David Kopečný, Francesca Pierigè, Mauro Magnani, Rosella Mollicone, Farhad Haghighi-Rad, Yann Gaston-Mathé, Julien Dairou, Claude Boucheix, and Raphaël Saffroy.

Affiliations: Assistance Publique-Hôpitaux de Paris, Hospital Paul-Brousse, Villejuif, France (D.M., E.G., R.S, J.H.); INSERM U935, Villejuif, France (D.M., F.H.-R., C.D., C.B.); University Paris-Sud, Villejuif, France (D.M., R.M., J.H., F.H.-R., C.D., R.S., C.B.); University Paris-Saclay, Paris, France (D.M., R.M., J.H., F.H.-R., C.D., R.S., C.B.); University of Urbino *Carlo Bo*, Urbino, Italy (L.R., F.P., M.M.); INSERM U1193, Villejuif, France (J.H., R.S.); INSERM U1197, Villejuif, France (R.M.); INRA-AgroParisTech, UMR 782 GMPA, Thiverval-Grignon, France (P.Bo.); Institut Jean-Pierre Bourgin, INRA-AgroParisTech, University Paris-Saclay, Versailles, France (P.Br.); CRH-Department of Protein Biochemistry and Proteomics, Palacký University, Olomouc, Czech Republic (D.K.); YGM Consult SAS, Paris, France (Y.G.-M.); CNRS UMR 8601, Paris, France (J.D.); Assistance Publique-Hôpitaux de Paris, Hospital Necker-Enfants Malades, Paris. France (B.C.-V.); and University Paris-Descartes, Paris, France (J.D., B.C.-V.)

Corresponding author: David Machover, MD. Department of Medical Oncology. Hospital Paul-Brousse. 94800 Villejuif. France. Telephone: +33 (0)609436331. Fax: +33 (0)145593498. E-mail address: david.machover1@orange.fr ; david.machover@aphp.fr

Supplemental Table S1. Primers used for MassArray quantitative methylation analysis of promoter sequences of selected genes.[1]

Primer[2]	Sequence[1]
APAF1F	AGG-AAG-AGA-GAT-TAG-AGG-TGG-GGA-GTT-TGG-GTA-GT
APAF1R	CAG-TAA-TAC-GAC-TCA-CTA-TAG-GGA-GAA-GGC-TAC-CCC-ACT-ACT-AAA-CAC-AAA-AAA-AA
APAF12F	AGG-AAG-AGA-GGT-TTT-AGG-GTT-TTT-AGA-TAT-GTT-TGA-GGT
APAF12R	CAG-TAA-TAC-GAC-TCA-CTA-TAG-GGA-GAA-GGC-TTC-CAC-TTA-CCA-AAC-CAA-ACC-C
ATP10A2F	AGG-AAG-AGA-GGT-TTA-ATT-TAT-TTG-TTG-AAG-ATT-AGG-TAG-T
ATP10A2R	CAG-TAA-TAC-GAC-TCA-CTA-TAG-GGA-GAA-GGC-TTA-CTA-TCC-TTC-CTA-CCC-AAA-AAC-CTA-T
CA3F	AGG-AAG-AGA-GAA-ATT-TTG-TAG-TTT-TGA-GAG-AGA-AGA-AGA-G
CA3R	CAG-TAA-TAC-GAC-TCA-CTA-TAG-GGA-GAA-GGC-TAA-AAA-AAC-CAA-TAA-ATT-CCA-AAA-AC
CA32F	AGG-AAG-AGA-GGG-GTA-GAG-GAA-GTT-AAT-GAA-TTT-TAA-GAG
CA32R	CAG-TAA-TAC-GAC-TCA-CTA-TAG-GGA-GAA-GGC-TAA-AAA-ATA-AAA-AAA-CCA-AAA-ACC-AC
CD38F	AGG-AAG-AGA-GTT-TAT-TTT-AGG-ATG-AAT-TTT-AGT-GTA-TTT-G
CD38R	CAG-TAA-TAC-GAC-TCA-CTA-TAG-GGA-GAA-GGC-TAC-TCT-CTA-AAA-AAA-CCC-AAC-TCT-ATC-T
CDH1F	AGG-AAG-AGA-GGT-TGT-TGT-TGT-TGT-TGT-AGG-TAT-TT
CDH1R	CAG-TAA-TAC-GAC-TCA-CTA-TAG-GGA-GAA-GGC-TCC-CAC-TCC-CAT-CAC-TAA-AAA-ATC
CDH12F	AGG-AAG-AGA-GGT-TAA-AGT-TAG-GGT-GGT-AGG-GTT
CDH12R	CAG-TAA-TAC-GAC-TCA-CTA-TAG-GGA-GAA-GGC-TAC-TAA-AAT-CCT-CCC-CCA-ATC-CC
CDKN2AF	AGG-AAG-AGA-GAT-TTT-GTT-TTT-TAA-ATT-TTT-TGG-AGG-GAT
CDKN2AR	CAG-TAA-TAC-GAC-TCA-CTA-TAG-GGA-GAA-GGC-TAA-AAA-AAC-CCA-ATC-CTC-CTT-CCT-TAC
CCNB2F	AGG-AAG-AGA-GGG-TAT-TTG-AAT-TTT-GGA-ATA-AGG-TTA-TAG
CCNB2R	CAG-TAA-TAC-GAC-TCA-CTA-TAG-GGA-GAA-GGC-TAA-AAA-AAC-AAA-AAT-ACC-AAC-CC
CIDEAF	AGG-AAG-AGA-GGT-TGT-GAT-TTT-TAG-GAT-TTT-TAG-AAG-TT
CIDEAR	CAG-TAA-TAC-GAC-TCA-CTA-TAG-GGA-GAA-GGC-TAC-TAA-ACA-CAA-ATA-CCA-AAT-ATA-ACT-CTT-AC
DAPK1F	AGG-AAG-AGA-GAT-GTG-GTT-TTG-GGG-ATT-GTT-T
DAPK1R	CAG-TAA-TAC-GAC-TCA-CTA-TAG-GGA-GAA-GGC-TCA-ACT-TTC-CCA-CCT-CCA-AAA
DCCF	AGG-AAG-AGA-GGT-TTT-TGG-TTA-AAG-GAA-GAT-GAG-GAG-TT
DCCR	CAG-TAA-TAC-GAC-TCA-CTA-TAG-GGA-GAA-GGC-TTT-TCT-CTT-CTC-TAC-TAA-ATA-CTA-CAT-AAC-CAA
EGFRF	AGG-AAG-AGA-GTT-TTT-TTA-GTT-GTT-AGG-TTA-GTT-TTT-GA
EGFRR	CAG-TAA-TAC-GAC-TCA-CTA-TAG-GGA-GAA-GGC-TAC-CAA-ATC-TAT-ACC-AAA-ATC-CCC-TT
EGFR2F	AGG-AAG-AGA-GTA-GGG-AAG-TTG-AGG-AAG-GAA-TTT-A
EGFR2R	CAG-TAA-TAC-GAC-TCA-CTA-TAG-GGA-GAA-GGC-TAA-TTC-TCC-CAA-CTC-CCA-AAT-C
EGFR3F	AGG-AAG-AGA-GTA-AAG-TAA-ATT-TGT-ATT-AGT-TTT-AGA-TAG-ATT-GG
EGFR3R	CAG-TAA-TAC-GAC-TCA-CTA-TAG-GGA-GAA-GGC-TAA-CTA-CCA-AAC-CAA-CCT-CTA-ATC-CC
ESR1F	AGG-AAG-AGA-GTT-TTA-TTG-TAT-TAG-ATT-TAA-GGG-AA
ESR1R	CAG-TAA-TAC-GAC-TCA-CTA-TAG-GGA-GAA-GGC-TAC-TTA-CTA-CTA-TCC-AAA-TAC-ACC-TC
ESR12F	AGG-AAG-AGA-GGT-TAT-TTT-AGA-TGT-TTT-GGT-GTG-GAG-G
ESR12R	CAG-TAA-TAC-GAC-TCA-CTA-TAG-GGA-GAA-GGC-TAA-CTA-TAC-TCT-TTT-TCC-AAA-TAA-CCC
FHITF	AGG-AAG-AGA-GTT-TAT-TTT-TTA-GGA-TGT-TGA-TAG-TTG-GG
FHITR	CAG-TAA-TAC-GAC-TCA-CTA-TAG-GGA-GAA-GGC-TTA-AAA-TCT-TCT-AAA-AAT-TAC-AAT-CCC-C
FLT3F	AGG-AAG-AGA-GTT-TTT-TTT-AGA-GGT-AGG-GAT
FLT3R	CAG-TAA-TAC-GAC-TCA-CTA-TAG-GGA-GAA-GGC-TAA-AAC-TCA-CAA-AAA-CAA-CAA-AAC
FRAT1F	AGG-AAG-AGA-GTT-TTG-TAA-GTG-TTG-GAG-TTT-TTT-GAG
FRAT1R	CAG-TAA-TAC-GAC-TCA-CTA-TAG-GGA-GAA-GGC-TAA-AAA-ACC-CCT-TAC-CCT-CCA-ATC-TAC
GPC3F	AGG-AAG-AGA-GTA-TTT-TTA-AGT-GTT-TAG-TTG-TAG-GG
GPC3R	CAG-TAA-TAC-GAC-TCA-CTA-TAG-GGA-GAA-GGC-TAA-ATA-AAT-ACC-AAA-AAC-TCC-C
GSTP1F	AGG-AAG-AGA-GTA-GGG-GTT-GGG-GTT-GTA-GTT-TAT-AGT-T
GSTP1R	CAG-TAA-TAC-GAC-TCA-CTA-TAG-GGA-GAA-GGC-TAA-AAA-AAC-AAA-AAA-ACA-AAT-TCC-TCC
IRF4F	AGG-AAG-AGA-GGT-TAG-TTG-GGT-AGG-GAT-AGG-GGT-TTT-AT
IRF4R	CAG-TAA-TAC-GAC-TCA-CTA-TAG-GGA-GAA-GGC-TAC-TCT-ATC-AAT-TTC-CAC-TCC-CCT-AA
KLF11F	AGG-AAG-AGA-GGG-GAT-ATT-TAG-GTT-AAT-AAG-TTT-TGA-TTT-T
KLF11R	CAG-TAA-TAC-GAC-TCA-CTA-TAG-GGA-GAA-GGC-TAA-TTA-TTT-TTA-ACT-TCT-ATC-ATT-CTC-CCT-TC
KLF13F	AGG-AAG-AGA-GGT-GAG-AGT-TAA-GGG-TAA-GGT-GGT-TT
KLF13R	CAG-TAA-TAC-GAC-TCA-CTA-TAG-GGA-GAA-GGC-TCT-ACC-AAC-TCT-TCT-AAA-CTA-CCC-CTC-T
LMO2F	AGG-AAG-AGA-GGG-TAT-AGG-GGG-TTA-AGG-GTA
LMO2R	CAG-TAA-TAC-GAC-TCA-CTA-TAG-GGA-GAA-GGC-TAA-CCT-AAA-CCC-TTC-AAA-ATA-AAT-AC

MAD2L1F	AGG-AAG-AGA-GAT-GGT-TAG-GGA-TAT-AAA-TAA-AAG-TA
MAD2L1R	CAG-TAA-TAC-GAC-TCA-CTA-TAG-GGA-GAA-GGC-TAC-ATC-ACA-AAA-AAA-CTA-AAA-AAA-A
MAD2L12F	AGG-AAG-AGA-GAT-ATT-ATA-GGA-AGG-TTG-AGA-GAA-AGG-GTA-G
MAD2L12R	CAG-TAA-TAC-GAC-TCA-CTA-TAG-GGA-GAA-GGC-TCA-TAA-CCA-AAA-ACA-CAA-ACA-AAA-ACA-C
MAD2L2F	AGG-AAG-AGA-GAT-TTT-TTT-GGG-TAT-AGA-TGG-GA
MAD2L2R	CAG-TAA-TAC-GAC-TCA-CTA-TAG-GGA-GAA-GGC-TCT-CAA-ACA-AAA-AAC-CCC-AAT-CC
MGMTF	AGG-AAG-AGA-GTG-GTA-AAT-TAA-GGT-ATA-GAG-TTT-TAG-G
MGMTR	CAG-TAA-TAC-GAC-TCA-CTA-TAG-GGA-GAA-GGC-TAA-AAC-CTA-AAA-AAA-ACA-AAA-AAA-C
MLH1F	AGG-AAG-AGA-GGT-ATT-GAG-GTG-ATT-GGT-TGA-AGG-TAT-TTT
MLH1R	CAG-TAA-TAC-GAC-TCA-CTA-TAG-GGA-GAA-GGC-TAT-TCT-CAA-TCA-TCT-CTT-TAA-TAA-CAT-TAA-CT
MLH12F	AGG-AAG-AGA-GGG-TAT-TTT-TGT-TTT-TAT-TGG-TTG-GA
MLH12R	CAG-TAA-TAC-GAC-TCA-CTA-TAG-GGA-GAA-GGC-TCA-ACT-TAA-ATA-CCA-ATC-AAA-TTT-CTC-AA
MYOD1F	AGG-AAG-AGA-GTT-TTT-GTT-GTT-TGT-AGA-TGG-ATT-ATA-G
MYOD1R	CAG-TAA-TAC-GAC-TCA-CTA-TAG-GGA-GAA-GGC-TCC-TAA-ATA-AAA-ACC-AAA-ACA-ACT-CCA-TA
MYOD12F	AGG-AAG-AGA-GGG-TTG-TTT-AAG-GTG-GAG-ATT-TTG
MYOD12R	CAG-TAA-TAC-GAC-TCA-CTA-TAG-GGA-GAA-GGC-TCC-CTA-ACT-TCC-TCA-CTT-CCT-AAA-A
PEG3F	AGG-AAG-AGA-GGG-GAA-AGA-AAA-TTT-TTA-TAG-GTA-GGA-TAG-TT
PEG3R	CAG-TAA-TAC-GAC-TCA-CTA-TAG-GGA-GAA-GGC-TAA-AAC-CCT-AAA-CCT-CCT-AAA-CTA-AAT-CTA-A
PHOX2BF	AGG-AAG-AGA-GAT-TTT-TTT-TAG-TTT-TTT-GAG-TTG-GGT-ATT-G
PHOX2BR	CAG-TAA-TAC-GAC-TCA-CTA-TAG-GGA-GAA-GGC-TAT-AAC-CTA-ACC-TTA-AAA-TCC-TCA-CAT-TCT-A
PTPRN2F	AGG-AAG-AGA-GGT-TTT-AGG-GTT-AGG-GGA-GTG-T
PTPRN2R	CAG-TAA-TAC-GAC-TCA-CTA-TAG-GGA-GAA-GGC-TCA-AAC-TCT-AAA-TCT-CAA-ACC-CC
RASSF1AF	AGG-AAG-AGA-GGA-GAA-TGT-TTG-TAT-TGT-GGT-TTG-TTT-AT
RASSF1AR	CAG-TAA-TAC-GAC-TCA-CTA-TAG-GGA-GAA-GGC-TCT-ACA-AAT-TAC-AAA-TTC-ACC-TAC-CAC-TAC-C
RASSF1A2F	AGG-AAG-AGA-GTA-GTT-AGG-AGG-GTG-GGG-TTG-TTT-AT
RASSF1A2R	CAG-TAA-TAC-GAC-TCA-CTA-TAG-GGA-GAA-GGC-TAA-CAA-TAA-CTA-CTA-CAA-CCA-AAA-AAA-CT
SNRPNF	AGG-AAG-AGA-GGG-TTT-TAA-AGT-TTT-TTG-TTT-TGG-AG
SNRPNR	CAG-TAA-TAC-GAC-TCA-CTA-TAG-GGA-GAA-GGC-TAA-ACT-ACA-ATC-ACC-CTA-ATA-TAC-CCA-C
SALL1F	AGG-AAG-AGA-GAT-ATT-AAT-AAA-AAT-AGA-AGT-AGA-GTG-GGG-G
SALL1R	CAG-TAA-TAC-GAC-TCA-CTA-TAG-GGA-GAA-GGC-TAC-CTC-CAC-CCA-AAA-TTA-AAA-AAA-TAC-TAC
SALL3F	AGG-AAG-AGA-GAT-TTG-GAA-GTT-TTA-GAA-AGA-TTT-AAA-GAT-A
SALL3R	CAG-TAA-TAC-GAC-TCA-CTA-TAG-GGA-GAA-GGC-TAA-ACA-AAT-CCA-AAA-CCA-ACT-AAA-CTC
TLX3F	AGG-AAG-AGA-GGG-GAT-TTT-ATA-GTG-TGA-ATT-TGA-GTT-TA
TLX3R	CAG-TAA-TAC-GAC-TCA-CTA-TAG-GGA-GAA-GGC-TAC-TAC-TCT-CCA-TCC-AAA-AAA-AAT-TAA-AAC-C
TIMP3F	AGG-AAG-AGA-GGT-AGT-TGG-AGT-TTG-GGG-GAT-TG
TIMP3R	CAG-TAA-TAC-GAC-TCA-CTA-TAG-GGA-GAA-GGC-TCT-ACC-CCT-CTC-CTA-AAA-CAA-AAA-AA
TNFRSF10CF	AGG-AAG-AGA-GGG-TTT-TGT-TGT-TAG-TGA-GTT-T
TNFRSF10CR	CAG-TAA-TAC-GAC-TCA-CTA-TAG-GGA-GAA-GGC-TAA-ACC-CAA-TTC-TTC-CCC-TAA-CT
VIMF	AGG-AAG-AGA-GTT-TTT-TTT-GGT-AGG-TTG-TTA-ATT-AT
VIMR	CAG-TAA-TAC-GAC-TCA-CTA-TAG-GGA-GAA-GGC-TCA-ACT-TTC-AAA-CCT-ACT-ACC-CTC
VIM2F	AGG-AAG-AGA-GGT-TTA-TTT-TGG-GGT-GTT-GAA-AAA-GG
VIM2R	CAG-TAA-TAC-GAC-TCA-CTA-TAG-GGA-GAA-GGC-TAT-CTA-AAA-AAT-TCC-TTA-CTC-TTT-CCT-CTT-C
TP53INP1F	AGG-AAG-AGA-GGT-TTA-ATT-TTA-GGT-TGA-TTA-GGT-GGG
TP53INP1R	CAG-TAA-TAC-GAC-TCA-CTA-TAG-GGA-GAA-GGC-TAA-AAA-AAC-AAA-AAT-AAA-TCT-CTC-CCT-CAA-C
TLX32F	AGG-AAG-AGA-GGT-TGT-GTG-TTA-GAG-GGT-TTT-TAG-GAG
TLX32R	CAG-TAA-TAC-GAC-TCA-CTA-TAG-GGA-GAA-GGC-TAA-TAA-TAC-AAA-ACC-AAC-CTA-CTC-ACC-C

[1]Amplicons and PCR primers were designed using the website http://agenacx.com/epidesigner/

[2]Letters F and R at end of each primer name indicate forward and reverse, respectively.

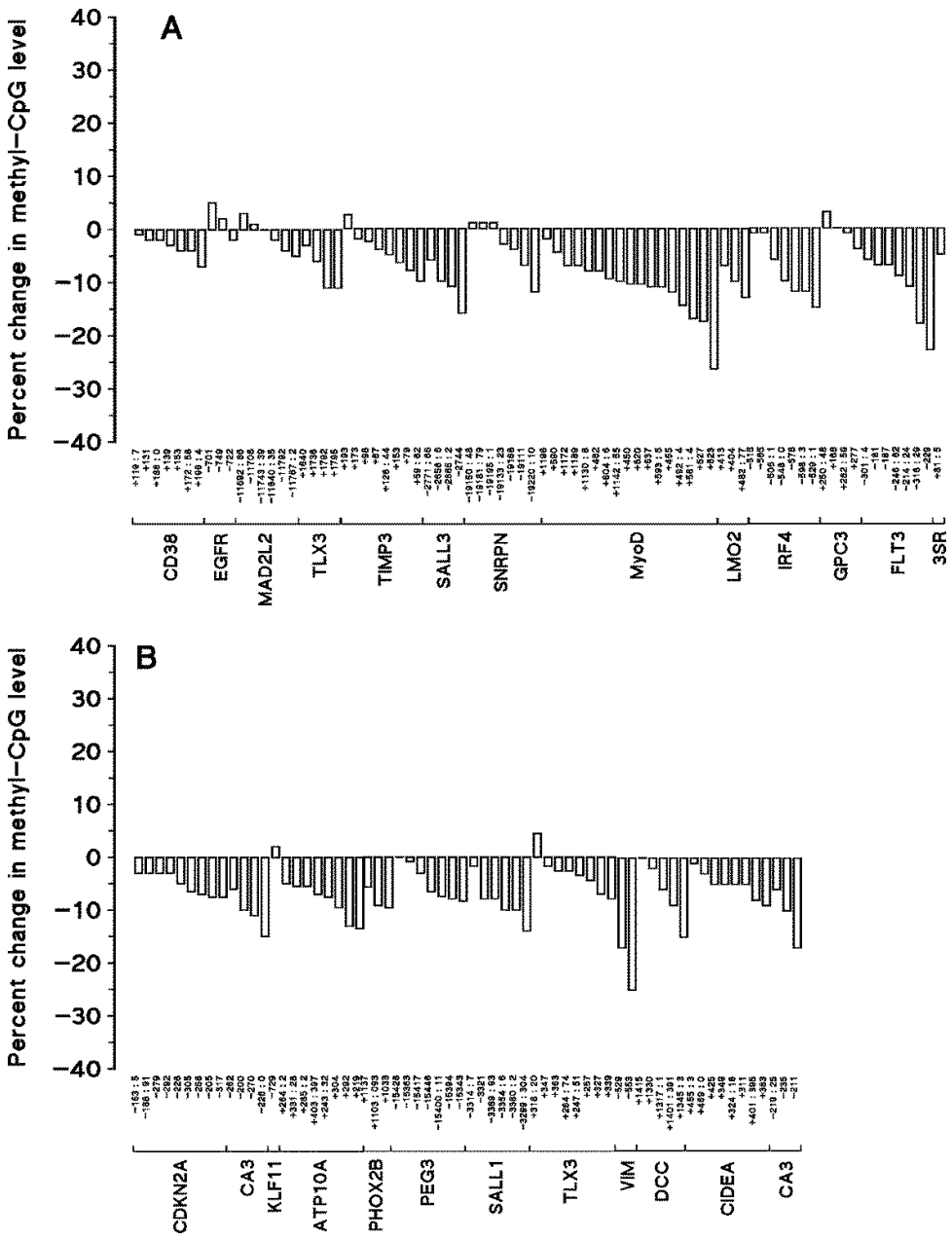

Supplemental Figure S1. Mean methyl-CpG percent change from control of gene promoters in colorectal cancer HT29 cells exposed to MGL-BL929 at 1 Unit/ml for 72 hours. Methylation rates in fragments with a single CpG or groups of 2 to 5 contiguous CpGs were measured in 142 DNA fragments comprising 229 CpG dinucleotides whose baseline methyl-CpG levels in control cells were greater than 70% (mean percent methyl-CpG, 88.64). Bars in Figures A and B represent the difference in mean methyl-CpG level of fragments in cells exposed to the MGL-BL929 and that in control cells unexposed to the enzyme. Numbers under bars indicate positions from the first nucleotide of coding DNA sequences to each single 5-meC or groups of 5-meCs within CpG dinucleotides of gene promoters. The difference between percent methylation in paired samples was statistically significant (Two-sided Wilcoxon Rank-Sum Test, $***P = 1.3\text{x}10^{-9}$).